



COMMISSARIAT À L'ÉNERGIE ATOMIQUE

# DSM - DAPNIA

DIRECTION DES SCIENCES DE LA MATIÈRE

DEPARTEMENT D'ASTROPHYSIQUE, DE PHYSIQUE DES PARTICULES, DE  
PHYSIQUE NUCLÉAIRE ET DE L'INSTRUMENTATION ASSOCIÉE

## SACM

SERVICE ACCÉLÉRATEURS CRYOMODULES ET  
MAGNETISMES

N/RÉF : DSM/DAPNIA/SACM 02/XX

V/RÉF :

OBJET : IFMIF KEP summary report

# IFMIF KEP Phase CEA-Saclay summary report

1	AC11A-EU-CEA-Saclay : Very long test of ion source.....	3
1.1	Brief task description.....	3
1.2	Contributors.....	3
1.3	Introduction.....	3
1.4	Summary of the first run tests .....	3
1.5	First four weeks reliability test.....	3
1.6	New long run.....	5
1.7	One month reliability test.....	5
1.8	Conclusion .....	6
1.9	References .....	6
2	AC12A-AC13A-AC14-EU-CEA-Saclay : ECR Source analyses .....	7
2.1	Brief task description.....	7
2.2	Deuteron performance of ECR source.....	7
2.3	Species fraction.....	8
2.4	Beam noise measurement.....	8
2.5	Activation .....	9
2.6	Emittance measurement.....	9
2.7	Space charge measurements.....	10
2.8	SILHI Status .....	12
2.9	Conclusion .....	12

2.10	References .....	13
3	AC21A-EU-CEA-Saclay : Radio frequency system.....	14
3.1	Brief task description.....	14
3.2	Contributors.....	14
3.3	Introduction.....	14
3.4	Conclusion .....	16
3.5	References .....	16
4	AC33A, AC38 -EU-CEA-Saclay: End to End beam dynamics .....	17
4.1	Brief task description.....	17
4.2	Contributors.....	17
4.3	Introduction.....	17
4.4	RFQ design.....	17
4.5	DTL design.....	18
4.6	Errors Studies .....	19
4.7	Conclusion and perspective .....	20
4.8	References .....	20
5	AC34-EU-CEA-Saclay : RFQ Tuning method, Electric field optimisation on cold model..	22
5.1	Brief task description.....	22
5.2	Contributors.....	22
5.3	Studies.....	22
5.4	Conclusion .....	24
5.5	References .....	25
6	AC36-EU-CEA-Saclay : Drift Tube Linac R&D Studies .....	26
6.1	Brief task description.....	26
6.2	Contributors.....	26
6.3	Introduction.....	26
6.4	Magnets .....	26
6.5	Drift tubes.....	27
6.6	Tank design.....	28
6.7	Hot model tests.....	29
6.8	Perspectives.....	29
6.9	References .....	29
7	AC41-EU-CEA-Saclay : Diagnostics for high power beam.....	30
7.1	Brief task description.....	30
7.2	Contributors.....	30
7.3	Introduction.....	30
7.4	Optical measurement .....	30
7.5	Shifted doppler fluorescence beam profile measurements (SDFBPM).....	31
7.6	Interceptive profile measurement methods.....	32
7.7	Experiments with wire scanner. ....	33
7.8	Conclusion .....	34
7.9	References .....	34

## 1 AC11A-EU-CEA-Saclay : Very long test of ion source

### 1.1 Brief task description

The task was completed in the framework of the CEA program on high-power particle accelerators supported by the IPHI demonstrator project. This project is dedicated to high power beam production (CW beam, 100 mA).

The injector system (source and Low Energy Beam Transport) must demonstrate reliability commensurate the maintenance schedule of the IFMIF accelerators. Low to very low spark rates have to be shown, as well as reliability in terms of source performances.

The work concentrated on verifying/improving the ECR source availability on a 100 mA beam for more than 4 weeks. Current, beam energy, beam noise, species fraction, beam emittance... were recorded. The source ran in a proton mode to avoid activation of the existing test stand.

### 1.2 Contributors

Name	Party	Institute	E-mail address
R. Ferdinand	EU-FRANCE	CEA-Saclay	<a href="mailto:rferdinand@cea.fr">rferdinand@cea.fr</a>
R. Gobin	EU-FRANCE	CEA-Saclay	<a href="mailto:rjgobin@cea.fr">rjgobin@cea.fr</a>

### 1.3 Introduction

SILHI (“Source d’Ions Legers Haute Intensité”) is in operation at CEA-Saclay. It delivered its first proton beam in July 1996. This ECR (Electron Cyclotron Resonance) source is designed to produce continuous high-intensity proton and deuteron beams. The reliability-availability is one of the most important goals. So the source has to be as reliable as possible and 6 long run tests have been done to analyse its behaviour in continuous operation.

The extraction system has been improved in the past to minimize beam losses at higher extracted beam current and the source command and control system was completely updated with the EPICS system. This new configuration allows us to extract higher intensity deuteron beam after conditioning, a second long run reliability test has been performed for 1 month in October 2001.

### 1.4 Summary of the first run tests

In December 1997 the source has been continuously operated during 5 days (103 hours) with a 100 mA CW proton beam at 80 keV. The global reliability reached 94.5 % with 53 shutdowns mainly induced by HV sparks. The second test has been performed in May 1999 with a 75 mA CW beam at 95 keV, the availability reached 98 % for a continuous operation of 106 hours. The beam has been interrupted 24 times.

In October 1999, after improvements, a new 5 days test run was done with a 75 mA extracted beam at 95 keV. **Only one beam trip occurred during the 104 hours run test for 2'30" and 103 hours uninterrupted running time have been achieved. The reliability reached 99.96 %.**

### 1.5 First four weeks reliability test

Long run tests often benefit the knowledge of the source behaviour and component failure. A four weeks run test has been decided following the remote control exchange and the installation of the new extraction system.

To limit beam losses in the extraction zone, a new set of electrodes has been designed and assembled on the installation in October 2000; it allows us to extract up to 150 mA total extracted beam with a LEBT transparency (up to the future RFQ matching point) higher than 90 %.

Then the source was stopped for 2.5 months (mid of November 2000 to end of January 2001) to completely change the remote control system. The old one, based on Visual Basic and PCs, controlled all the power supplies and was associated with a Selectron PLC for vacuum control. The SILHI source became the development test bench of this EPICS system. It was also the only way to make a 4 weeks

run and with accurate beam characteristics measurements. It includes much better automatic recovery system. At the end of January, the beam was again extracted and weeks have been spent to improve the control system, specifically the automatic procedures. These procedures allow us to leave the source working without any operator and allow long distance control through modem connections. For the new long run test, all beam characteristics were checked: beam intensity, proton fraction, emittance and beam noise. To avoid LEBT activation, the tests were made with protons. The 4 weeks run started on Monday March 19, 2001 with the beam parameters reported in Table 1

Table 1: SILHI 1<sup>st</sup> long run requirements and run test parameters

Parameters	Requests	Run Status
Energy [keV]	95	95
Proton extracted beam [mA]	100	≈ 97
Total extracted beam [mA]	110	118
Proton fraction [%]	> 90	≈ 84
Extraction aperture [mm]	9	9
Extracted beam density [mA/cm <sup>2</sup> ]	156	185
Forward RF power [W]	Up to 1200	1000
Duty cycle [%]	100	100
Hydrogen mass flow [sccm]	< 10	5.3
Beam noise (rms) [%]	< ± 1	± 0.95 max

Due to various problems, the experiment has been definitely interrupted on Monday April 09 in the morning for a complete check-up of the accelerator column. Unless what was expected, we were not able to run with a satisfactory source behaviour. Even if this reliability test did not reach the expected results, it gave us lots of information summarized hereinafter.

- Beam line pollution leads to rapid beam quality degradation. The LEBT design has to clearly take this into account.
- The O<sub>2</sub> cleaning beam seems very efficient to improve the proton fraction but unfortunately after the cleaning, the spark rate increased. The improvement of proton fraction after ion source conditioning with oxygen plasma is similar if not identical to Los Alamos LEDA injector performance.
- The automatic restart procedures were not completely well adapted to all the situations especially if a spark occurs during the restart period. Improvements were done to minimize these failures. An automatic restart presently takes 1 minute with a 1 second scan period.
- The new EPICS control system allowed us to work without any operator locally and to operate with home connection via Internet network if needed. Only few hardware failures obligate us to come back to the source to repair. Despite this good control system, spark during week-end and night implied very long beam stop. It necessary decreased the beam availability. A better operability could be obtained with 24 h a day in-situ control.
- The servo control loop, which maintains a constant extracted beam current, works well.
- The beam noise was never over ± 0.95 % and frequently in the ± 0.5 to ± 0.7 % range. This noise was mainly due to the 19 kHz spaced-lines transferred to the plasma from the magnetron RF switched power supply.

This 4-week reliability run test did not show the expected results for several reasons, including oil contamination. Compare to the 1999 tests, the main differences came from current increased and the new electrodes. With the new set of extraction electrodes, 100 mA proton beam are transported up to the future RFQ matching point and more than 150 mA total beam was extracted. The new set of electrodes increases by 10% the electric field at the surface. This may be one of the reasons of the spark rate increase. Of course, the pollution observed (carbon traces) is also very important for HV column reliability.

## 1.6 New long run

Soon after the failure of the 4-weeks run, and after improvements on the command/control system and the source itself, a new long run was started. Slightly more than a week time was then available, given about 160h of source availability. The results shown in Figure 1 give back the very good results of the October 1999 test, and reflect very well the today's source behaviour. We have about one spark per day. The MTBF was about 23 hours and the MTTR was about 2.5 min.

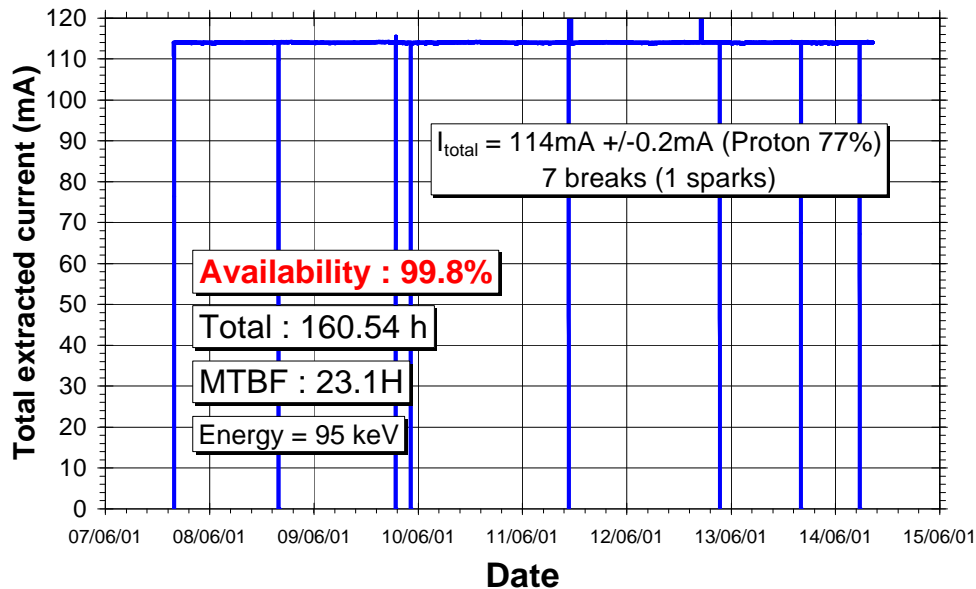


Figure 1 : total extracted beam current during the 160h long run tests of the CEA-Saclay ECR SILHI Source.

## 1.7 One month reliability test

A four weeks run test has been restart in October 2001, according to the decision taken in March 2001. The new procedures allow us to leave the source working without any operator and allow long distance control through modem connections.

Table 2 : SILHI 2<sup>nd</sup> long run requirements and run test parameters

Parameters	Requests	Run Status
Energy [keV]	95	95
Proton extracted beam [mA]	100	≈ 96
Total extracted beam [mA]	110	120
Proton fraction [%]	> 90	≈ 80
Extraction aperture [mm]	9	9
Extracted beam density [mA/cm <sup>2</sup> ]	156	185
Forward RF power [W]	Up to 1200	800
Duty cycle [%]	100	100
Hydrogen mass flow [scm]	< 10	5.7
Beam noise (rms) [%]	< ± 1	0.8 max

The 4 weeks run started on Monday October 5, 2001 with the beam parameters reported in Table 2. It last in fact for a full month through November 6 (744 hours). 233 sparks were recorded. The availability is equal to 95%. One big problem occurs in the beginning. No special technical point was related to this break down. A non-foreseen stop occurs on the VME during the weekend and nobody was present to restart the source. 15 hours of down time results of that specific problem. The availability would have increase to 97% without this 15 hours down time. The beam noise was

relatively stable in the range 0.5 to 0.8% total. The proton fraction increased from 77% to 81% during the month.

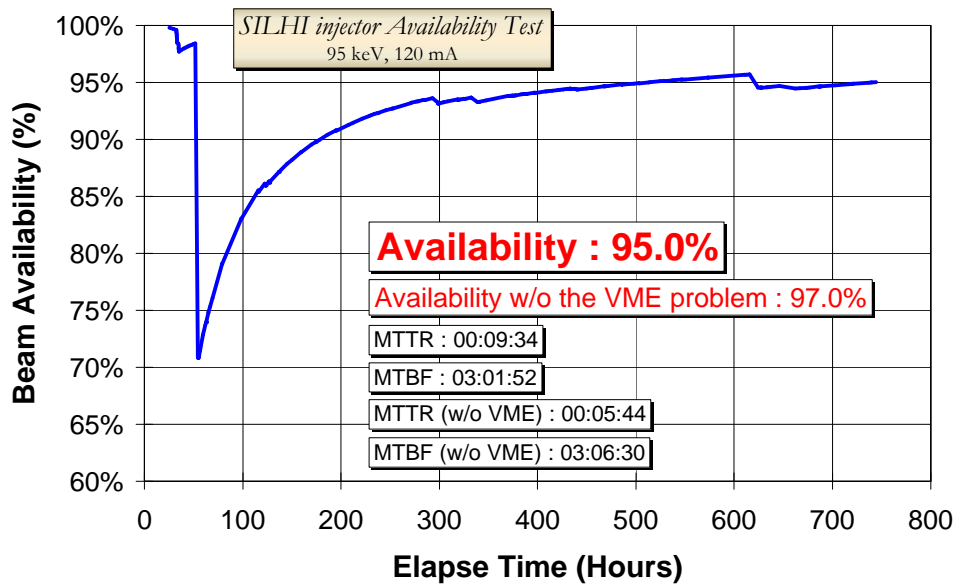


Figure 2 : Beam availability chart of the one month run test of the ECR SILHI source.

## 1.8 Conclusion

Most probably because of oil pollution in the source, the 2 very long runs did not give extremely good results. The most representative source behaviour was observed during the 160 hours test. We generally observe about one spark a day.

Nevertheless, IFMIF may have to take into account possible source malfunction. Some might be prevented with a careful design (screw pump, without oil for example).

## 1.9 References

- [1] R. Gobin, P-Y Beauvais, D. Bogard, R. Ferdinand, P. Mattéi, "Reliability tests of the high power proton source SILHI at CEA/Saclay", 3th international workshop on HPPA reliability, Santa Fe, USA, May 2002
- [2] R. Gobin, P.-Y. Beauvais, K. Benmeziane, D. Bogard, G. Charruau, D. De Menezes, O. Delferrière, R. Ferdinand, A. France, Y. Gauthier, F. Harrault, J.-L. Jannin, J.-M. Lagniel, P. Mattéi, A. Sinanna, P. Ausset, S. Bousson, D. Gardes, B. Pottin, L. Celona, J.D. Sherman, "Saclay High Intensity Light Ion Source Status", EPAC 2002, La villette PARIS 2002, page 1712
- [3] R. Ferdinand, P.-Y. Beauvais, A. France, R. Gobin, J.-M. Lagniel, "Deuteron Beam Test For IFMIF", EPAC 2002, La villette PARIS 2002, page 894.
- [4] R. Gobin et al., "High intensity ECR ion source (H+, D+, H-) developments at CEA Saclay", ISIS2001 conference, RSI, Vol.73, n°2, February 2002 (922)
- [5] P.-Y. Beauvais & al., "Status Report on the Saclay High Intensity Proton Injector Project (IPHI), EPAC 2000 Proceedings.

## 2 AC12A-AC13A-AC14-EU-CEA-Saclay : ECR Source analyses

### 2.1 Brief task description

The task was completed in the framework of the CEA program on high-power particle accelerators supported by the IPHI demonstrator project. This project is dedicated to high power beam production (CW beam, 100 mA).

The injector system (source and Low Energy Beam Transport) must demonstrate reliability commensurate the maintenance schedule of the IFMIF accelerators. Low to very low spark rates have to be shown, as well as reliability in terms of source performances. Very good beam quality has to be provided in order to ensure proper beam transport in the next accelerator sections. The task consists in analysing the source performance, and develops the necessary engineering. The source parameters that need to be obtained/verified are the total extracted  $D^+$  beam current at the IFMIF extraction energy, beam emittance, beam noise, pulsed and CW  $H^+$  operation. It is a continuous work that influences the accelerator parameters choice and could lead to cost saving (ex: if the emittance is decreased in the RFQ, the total RFQ length could be reduced, leading to a lower power consumption in the copper).

### 2.2 Deuteron performance of ECR source

Neutron production was foreseen in the Low Energy Beam Transport (LEBT) line. The authorization to extract a pulsed deuteron beam from the CEA-Saclay ECR source SILHI has been obtained in June 2001 based on our experiment on the Saturne accelerator. At that time the duoplasmatron source was delivering up to 50 mA of deuteron at an energy up to 500 keV (1ms, 1Hz) without observing neutron production. On IPHI test stand, to minimize the neutron production (d,D reaction) the source was in pulsed running mode (2ms/s) with lots of voluntary breaks to minimize the activation. The experiment was done using the 120 mA proton extraction system and bad extraction condition in deuteron was expected.

We observed excellent running conditions; SILHI source looks as well adapted for deuteron production as for protons. The source behaviour was very close to the proton production. In the effort to extract the maximum  $D^+$  beam current up to 170 mA was obtained at 100 keV (267 mA/cm<sup>2</sup>), but with an ugly shape and a lot of beam noise (Figure 3).

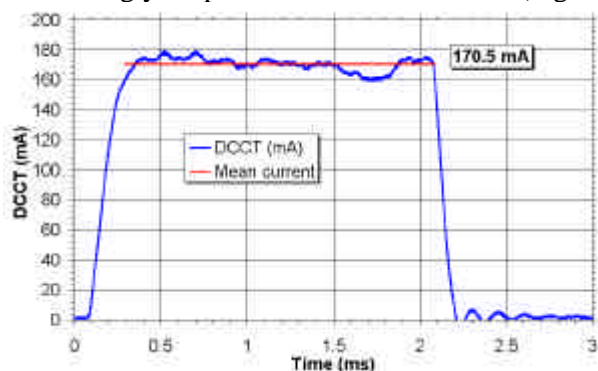


Figure 3: max extracted deuteron beam

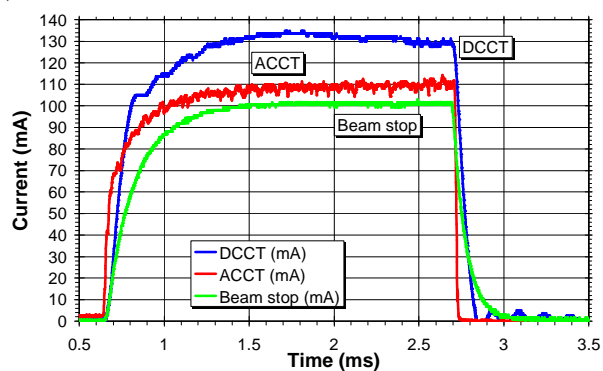


Figure 4 : 130 mA  $D^+$  beam through the LEBT

A more coherent set of measurements was seek in order to get a good qualification of the "normal" beam characteristics. It consists in tuning the source in good running condition and doing simultaneously all the possible measurements. The results are:

- $I > 130$  mA (100 kV)
- $D^+ > 96$  % and  $D_2^+ < 4$  % no measurable  $D_3^+$ .
- LEBT transparency = 75 %
- rms beam noise = 1.2 % (19 kHz)

Figure 4 shows the pulse measurement through the SILHI LEBT. In blue is the DCCT measurement of the extracted beam in the accelerator column. In red is the ACCT measurement, showing a better rising time since it has a much better bandwidth (see the beam noise paragraph). It shows also about 13% of beam loss at that point. This is due to the extraction electrodes adapted to a 120 mA proton beam. The last green curve is the beam stop measurement 4.4 m downstream the extraction aperture. It shows again some losses and the global LEBT transparency is only 75 %. This can be easily corrected to reach 100% with the appropriate set of electrodes. The rising time of the beam stop measurement is very low because of a filter on the faraday cup.

### 2.3 Species fraction

SILHI source is equipped with 3 different species fraction measurement techniques. The most useful one is the Wien filter, part of the emittance measurement unit. The beam is stopped on a water-cooled copper target with a small tantalum aperture. Behind, a Wien filter selects the species and they are analysed on a biased wire. Figure 5 shows the measurement associated with the “coherent set of measurement” described above.

The 2 other techniques are a classical aperture-faraday cup measurement and a non-interceptive Doppler shift measurement.

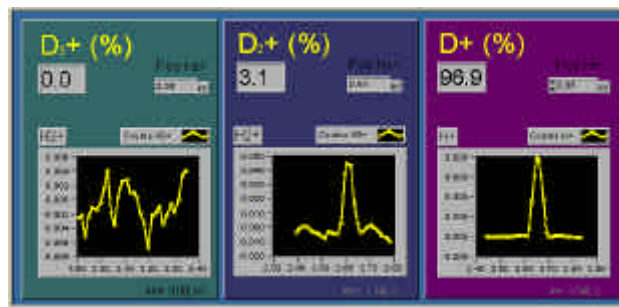


Figure 5 : typical deuteron proportion.

The 96.9% of  $D^+$  species is much better than the classical 80% usually obtained in CW proton mode. In pulsed mode, the source is tuned with a lower gas pressure allowing the species fraction to increase. Nevertheless, measurements in pulsed proton beam show that the species fraction is always better in deuteron production (96%) compared to proton production (92%). This observation is not yet understood.

### 2.4 Beam noise measurement.

The beam noise is measured using a 6MHz bandwidth ACCT, located between the 2 solenoids (about 2m downstream the aperture). Depending on the source tuning (pressure, ECR solenoid setting...) the rms beam noise is easily around 1.0% for good extraction condition ( $80 < I_{\text{beam}} < 130 \text{mA}$  @ 100keV). This noise was deeply analysed, and is mostly due to the 19 kHz spaced lines induced by the magnetron power supply. Time raster plots are used to display long signal records versus time, and allow :

- Detection of isolated, out-of-range samples,
- Detection of minute, periodic pulses,
- De-interleaving of multiple pulse bursts

Accelerators people need a good qualification of the noise. They need to know not only the rms value but also the probability distribution function to which the numbers of noise random processes apply. Figure 6 shows such probability function, and one of the important point is to notice the deviation from a symmetrical signal (left picture) and the deviation from a Gaussian signal (right picture).

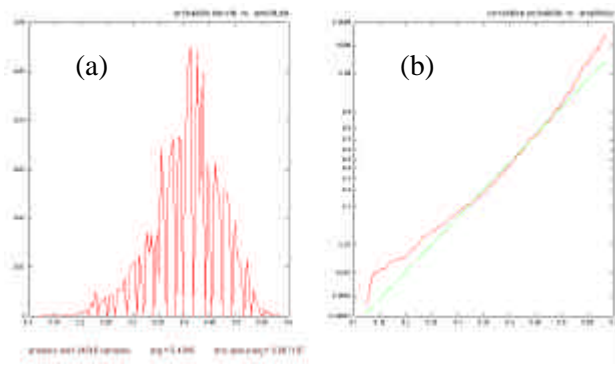


Figure 6 : (a) probability distribution function of the deuteron beam noise (1.2% in this case); (b) deviation from a Gaussian distribution represented by the green line

Checking noise amplitude distribution allow to :

- identify unsuspected noise sources,
- tune precisely the dynamic range of ADC's
- check for the linearity of these ADC's,
- quantify accurately the signal-to-noise ratio of the measurements.

The above results give an absolute value of rms beam noise compared to a “plus or minus” value, incompatible with the non-symmetrical distribution of the noise.

## 2.5 Activation

We ran the source in deuteron mode for 2 days, 0.2% dc, with lots of voluntary breaks to minimize the activation. During the test, high-energy neutron production was checked with a specific probe (Bertold LB 6411). The observed reaction is the (d,D) reaction at the surface of the copper target, producing 2.45 MeV neutrons. Unless what was expected, the activation linearly and quickly increased to reach 11.5  $\mu\text{Sv/h}$  ( $1.15 \text{ mrem.h}^{-1}$ ) after 2 hours (measured 60 cm from the target). The saturation level was not reached at that time, but the level was already above the workers class B in CEA.

The neutron production is highly dependant on LEBT pressure (around  $2 \times 10^{-5}$  torr during the test) and this is the explanation of the difference between the Saturne duoplasmatron and SILHI sources. Fortunately, the neutron production stops with the beam (no detection without beam) and no activation was observed close to the target switching back to protons. It may become a serious problem for CW accelerator (IFMIF) on a mid to long-term scale because of the species fraction ( $\text{D}_2^+$  and  $\text{D}_3^+$  lost on the vacuum pipe).

The observed level of neutron production forced us to run in a discontinuous mode, stopping as often as possible. Each restart of the source resumes the neutron production to the previous level. The night gives only very little decrease in this production, while running a few moments in CW proton mode cleaned the surface by a heating process.

## 2.6 Emittance measurement.

The beam r-r' emittance can be measured in 2 different locations: 53cm downstream the aperture or 4.4m downstream. Because of the activation, this measurement cannot be performed in deuteron, but only with the proton beam. Similar results are expected in deuteron production (emittance at the source exit is mostly defined by the extraction system)

At the source exit (0.53m) the beam emittance is in the range 0.155-0.175  $\pi \cdot \text{mm} \cdot \text{mrad}$  rms, normalized (r,r'). More important from the RFQ point of view, 99% of the beam is inside 1.4  $\pi \cdot \text{mm} \cdot \text{mrad}$ .

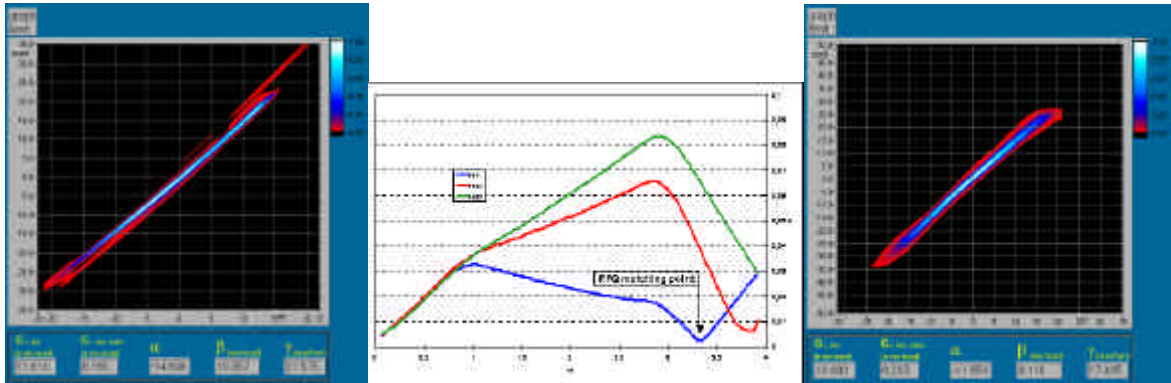


Figure 7 : Total normalised emittance of a 120mA proton beam@95keV, left at the source exit, right at the LEBT exit. Middle is the beam envelop calculation in the measurement configuration showing a cross over before the measurement.

Complete analyses of the beam emittance were done as a function of the source parameters. Extraction simulations indicated minimum emittance value for a 40 kV first gap extraction voltage, and this was confirmed by the measurements.

Beam emittance at the LEBT end depends on solenoids values and looks quite stable versus the extraction electric field configuration. It range at the LEBT end from 0.2 to 0.45  $\pi$ .mm.mrad (r-r', rms, normalised).

## 2.7 Space charge measurements

The high intensity beam induces ionisation of the residual gas, leading to space charge compensation [6]. In order to easily transport and match the proton beam at the RFQ entrance, the compensation has to be as high as possible.

A space charge analyser has been installed in the LEBT in order to measure the space charge compensation (SCC) of the beam. The description is given elsewhere [6] and it has been successfully used on different beams, especially on the LEDA injector (75 keV, 110 mA, CW). At Saclay, the FGA has been installed upstream and downstream the first LEBT solenoid (64 and 170 cm from the source aperture). It provides the ion energy distribution as well as the SCC.

### 2.7.1 Upstream Results

The SCC measurements lead to values of about 98 % for a beam current ranging from 60 to 100 mA. Different measures have been realized as function of beam energy, beam size, beam current and pressure.

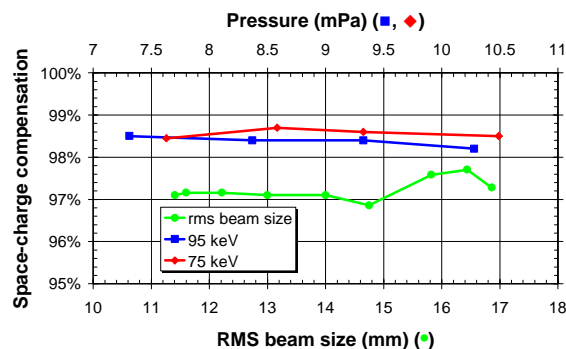


Figure 8 : SCC versus pressure, beam size and beam energy.

Beam size has been modified by varying the intermediate electrode potential. The rms beam size was ranging from 11 mm to 17 mm. The pressure curves were obtained by adding Argon or Hydrogen gas into the LEBT line. The residual gas pressure, measured close to the SCC analyser, was about  $4 \cdot 10^{-5}$  torr of mostly  $H_2$  without gas addition.

Figure 8 shows the condensed results as function of those parameters. The SSC ratio remains constant around 98% whatever the gas added or pressure and energy settings. Mostly the results are exactly the same as the ones obtained at LANL and the SCC is extremely good. At this point, no variation was observed that could explain the observed emittance reduction with gas injection.

### 2.7.2 Downstream results

The LEBT solenoid 1 allows a beam size change in a large range. A cross over of a few mm can easily be achieved for the  $H^+$  beam in front of the SCC analyser. Even the  $H_2^+$  becomes convergent. Depending on the settings, the SCC results changed a lot from the upstream results. Three peaks are commonly observed on the ions energy distribution curves that are attributed to the 3 separate beams  $H^+$ ,  $H_2^+$  and  $H_3^+$ . Analyzes are much more complicated and delicate in some cases.

#### Beam stop influence

A beam stop (BS) can be inserted 27 cm behind the FGA. There is no suppression of the secondary electrons (electrostatic or magnetic). These electrons are free to stream off into the beam plasma and affect the SSC degree.

When the BS is inserted, a lot of secondary electrons are produced and the SCC is about 98 %. This value decreases to about 80 % without the BS and an energy increase of the residual ions is observed. This energy shift is theoretically expected as the apparent current increases. Similar results are obtained depending on how much beam current is lost on the wall (low LEBT solenoid settings, steering on...).

When the second LEBT solenoid is on, a SCC increase is observed. These observations show that the solenoids play an important role of electrons confinement in the LEBT.

To achieve reliable SCC measurements it has been decided to make all the following experiments with the beam stop inserted into the LEBT line. In such conditions, the amount of free electrons created between the 2 solenoids remains almost constant for all the settings.

#### Pressure Influence.

Gas addition shows different results at this FGA location. Now the SCC increases from 89 % to 98 % with an Argon increase from  $4.3 \cdot 10^{-5}$  torr to  $8.1 \cdot 10^{-5}$  torr which means a factor 5 gain on the SCC (Figure 9).

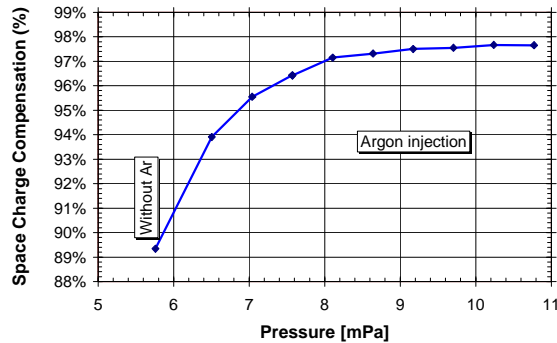


Figure 9 : SCC as a function of Argon addition in the LEBT.

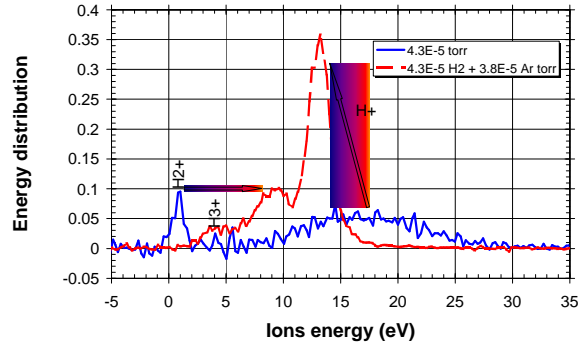


Figure 10 : Energy distribution function of the residual ions.

That phenomenon was NOT observed upstream the 1<sup>st</sup> solenoid and could explain the emittance decrease as the Argon pressure increases. Preliminary simulations using a basic model acknowledge that result, including that the Twiss parameters of the beam do not change a lot with the SCC after the solenoid.

The apparition of the  $H_2$  and  $H_3$  peaks on the energy distribution function could allow a rough estimation of the proton fraction (Figure 10).

### Beam size influence.

At this SCC analyser location, the rms beam size can easily be changed by a factor of 20. The results show a big change expected by the SCC theory in such extreme conditions.

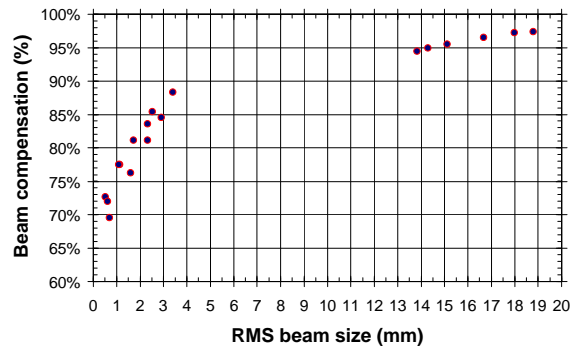


Figure 11 : SCC versus the rms beam size.

This SCC collapses in the vicinity of the cross over and leads to a large emittance increase (0.7 to  $1 \pi$ .mm.mrad rms values !)

### 2.7.3 Conclusion on space charge measurements.

A strong dependence on the number of free electrons in the LEBT line was found, as well as a mirror effect of the LEBT solenoids on those electrons. The SCC can be much lower than expected without an electron source such as occurs at the beam stop or due to beam losses on the beam pipe or induced by a pressure increase. Low SSC leads to a strong emittance increase in the LEBT.

## 2.8 SILHI Status

The following table brings a coherent set of parameters obtained all in once (except for the  $I_{max}$  quoted in bold after the total current)

Parameters	Proton		deuteron	
	Requests	Status	Request	Status
Energy [keV]	95	95	95	100
Intermediate Electrode [kV]	55	56	?	50
Proton, Deuteron Current [mA]	100	108	140	129
Total Current [mA] ( <b><math>I_{max}</math></b> )	110	130 ( <b>157*</b> )	155	135 ( <b>170</b> )
Proton, Deuteron Fraction [%]	> 90	83	> 90	96
Plasma electrode diameter [mm]	-	9	-	9
Current Density [mA/cm <sup>2</sup> ]	140	204	243	212
Availability [%]	AHAP	> 99	AHAP	-
RF Forward Power [W]	< 1200	850	< 1200	900
Duty Factor [%]	100	100	100	0.2 **
H <sub>2</sub> , D <sub>2</sub> Gas Flow [sccm]	< 10	5	< 10	1
Beam Noise rms [%]	2	1.2	2	1.2
rms normalized emittance [ $\pi$ .mm.mrad]	0.2 (x,x')	0.25 (r,r')	0.2	-
Total normalized emittance [ $\pi$ .mm.mrad]	1.5	1.4	1.5	

\* Limited by the beam stop (power density exceeding the faraday cup capability)

\*\* Limited by neutron production

## 2.9 Conclusion

SILHI showed excellent running conditions in deuteron production. The source looks as well adapted for deuterons production as for protons, the behaviour being very close to the proton production. Up to 170 mA of deuteron beam was extracted in pulsed mode, and 130 mA in good condition. The neutron

production in the LEBT rises rapidly to a dangerous level, and may lead to difficulties in the final IFMIF factory.

## 2.10 References

- [1] R. Gobin, P.-Y. Beauvais, D. Bogard, R. Ferdinand, P. Mattéi, "Reliability tests of the high power proton source SILHI at CEA/Saclay", 3th international workshop on HPPA reliability, Santa Fe, USA, May 2002
- [2] R. Gobin, P.-Y. Beauvais, K. Benmeziane, D. Bogard, G. Charruau, D. De Menezes, O. Delferrière, R. Ferdinand, A. France, Y. Gauthier, F. Harrault, J.-L. Jannin, J.-M. Lagniel, P. Mattéi, A. Sinanna, P. Ausset, S. Bousson, D. Gardes, B. Pottin, L. Celona, J.D. Sherman, "Saclay High Intensity Light Ion Source Status", EPAC 2002, La villette PARIS 2002, page 1712
- [3] P. Ausset, S. Bousson, D. Gardes, A.C. Mueller, B. Pottin, R. Gobin, G. Belyaev, I. Roudskoy, "Transverse Beam Profile Measurements for High Power Proton Beams", EPAC 2002, La villette PARIS 2002, page 245
- [4] R. Ferdinand, P.-Y. Beauvais, A. France, R. Gobin, J.-M. Lagniel, "Deuteron Beam Test For IFMIF", EPAC 2002, La villette PARIS 2002, page 894.
- [5] P. Ausset, S. Bousson, D. Gardès, A.C. Mueller, B. Pottin, R. Gobin, G. Belyaev, I. Roudskoy, "Optical Transverse Beam Profile Measurements for High Power Proton Beams", EPAC 2002, La villette PARIS 2002, page 1840
- [6] R. Ferdinand et al., PAC 97 conference, Vancouver, May 12-16, 1997.
- [7] N. Rouvière, F. Dubois, R. Leplat, L. Vatrinet, R. Gobin, F. Harrault, P.A. Leroy, "Status of the Vacuum System for the IPHI Project", EPAC 2002, La villette PARIS 2002, page 2586
- [8] P.-Y. Beauvais et al., "Emittance improvement of the SILHI beam by gas Injection in the LEBT", ISIS99 conference, RSI, Vol.71, n°3, June 2000, (1413)
- [9] B. Pottin et al.: "Optical beam profiler for high current beams", EPAC 2000, Vienna, Austria
- [10] R. Gobin et al., "High intensity ECR ion source (H+, D+, H-) developments at CEA Saclay", ISIS2001 conference, RSI, Vol.73, n°2, February 2002 (922)

### 3 AC21A-EU-CEA-Saclay : Radio frequency system

#### 3.1 Brief task description

Development and testing of a 1 MW rf system was identified as the highest impact development item. Existing operating experience was for short period of time (1-8 hours). The rf amplifier power baseline of 1 MW insures that a competitive bid could be obtained from two manufacturers. Accomplishing a full-scale test of the first system would allow the remaining large procurement to be on a fixed-price basis.

The task consists in collecting information on the THALES Diacrode TH628 progress. The main task remained the 1000h rf test and required an upgrade of their existing test stand. The test was done using the present 200 MHz – 1 MW diacrode, knowing that a higher frequency is generally harder to develop. This existing diacrode could achieve the requirement without spending the amount of money in buying a non-existing 175 MHz diacrode.

#### 3.2 Contributors

Name	Party	Institute	E-mail address
R. Ferdinand	EU-FRANCE	CEA-Saclay	<a href="mailto:rferdinand@cea.fr">rferdinand@cea.fr</a>
E. Margoto	EU-FRANCE	THALES Electron devices	<a href="mailto:Eric.margoto@thales-electrondevices.com">Eric.margoto@thales-electrondevices.com</a>

#### 3.3 Introduction

Each IFMIF accelerator will require 11 high power RF stations (22 total). Each station will provide 1 MW of cw RF power at 175 MHz. Together, they will be required to provide a world record level of average RF power.

The size of the RF power system makes it a major contributor to the IFMIF capital cost. The RF power system will also be a primary contributor to the annual operating cost. First, it dominates IFMIF electricity consumption (>40 MWe for both accelerators). Second, because several of the major RF components have limited lifetime (e.g., 10,000 hour expected lifetime for tetrode power amplifier tubes, 20,000 hr expected for RF windows). The annual costs for component replacement and refurbishment will be comparable with other major elements of the operating cost.

Because all 11 RF power stations must be operational for an accelerator to operate, it follows that the reliability, availability and maintainability of the individual RF power stations will be of critical importance to achievement of IFMIF's overall availability goals. However, it is generally recognized that existing operating experience with tetrode-based RF power systems is not sufficient to provide a high level of confidence in the reliability and maintainability of RF power stations of the required power and frequency, operating in cw mode.

Validation of the design performance, reliability and maintainability of the RF power technology selected for IFMIF is a key objective. A secondary objective is the early identification of potential design improvements that will enhance the ultimate performance and availability of the IFMIF RF power system. Another objective is to reduce the cost of procuring the RF power system by achieving a firm basis for fixing the design early in the project.

The RF tubes needed for the IFMIF accelerator are declared to work at 175 MHz with 1.0 MW CW output power. Although there was no tubes on the market having proved their ability to operationally provide such performances, the development work did exist and the achievement of a long test was needed to demonstrate the operational feasibility of the envisaged IFMIF RF design.

Existing operating experience is for short period of time (1-8 hours). Therefore a test lasting 100 – 1000 hours would represent a decisive stage in the validation of the proposed IFMIF design. Accomplishing a full-scale test of the first system would allow the remaining large procurement to be on a fixed-price basis.

IFMIF requirement imply a long test to ensure the quality of the design.

### 3.3.1 Scope of the contract

Thales Electron Devices has developed a new kind of gridded tubes called DIACRODE which can overcome the limitations of the conventional tetrode, mainly the RF losses. As a result, the first tube allowing for 1 MW of cw rf power can be obtained at IFMIF frequency (175MHz).

The scope of the contract was to assess the feasibility of a RF tube operating in relevant IFMIF conditions (175-200 MHz, 1MW CW). The diacrode TH628 has been tested on a rf cavity design also by Thales Electron Device, the cavity and the diacrode being a whole.

The activities of the contract were divided into 3 phases. The contract was placed initially for the first phase.

#### 1<sup>st</sup> phase

Assemble the needed equipment for the test programs and install the RF sources in the test facility.

Perform operability tests, which contain:

- Operation of the RF source in the range 175 MHz-200 MHz (175 MHz -0 MHz/+25 MHz), knowing that the RF losses are the main losses, and are proportional to the power  $5/2$  of the frequency. This frequency shift used for the test provide a safety margin on results.
- Operation of the RF source at 1 MW  $\pm$  150 kW at 175 MHz or 900 kW  $\pm$  100 kW at 200 MHz (Demonstration of 1 MW cw output power into a matched load).
- Determination of the maximum RF power output and power transmission capabilities (subject to operating thermal, mechanical and electrical loads)
- Recognition of system instabilities,
- Reporting on intermittent HV arcing in RF system, causing accelerator system shutdown.

Provide intermediate and final reports of the various phases of the specified testing.

#### 2<sup>nd</sup> phase

Perform lifetime 89 RF hours' test (Demonstration of continuous operation for 89 RF hours at 1 MW level, CW).

#### 3<sup>rd</sup> phase

Perform lifetime 941 RF hours' test (Demonstration of discontinuous operation at 1 MW level, CW, for 941 RF hours or up to first tube/test stand breaks. Continuous operation time for each phase had to be longer than 60 hours. This did provide initial RAMI (Reliability, Availability, Maintainability, Inspectability) and lifetime information. Record of the maximum output RF in CW operation.)

### 3.3.2 Results

The first phase was fully achieved and the first intermediate report was submitted on 26 February 2002. The test bench was modified and the operability tests have been performed reaching the full output RF power of 1030 kW.

In the second phase continuous operation at 1 MW level for 89 RF hours have been demonstrated (second intermediate report submitted on 16 April 2002).

The third phase consisted in 12 continuous runs carried out for periods ranging from 65 hours up to 220 hours. The conditions selected to make this test were the best ones, the cathode being cycled at each restarting.

The output RF power was for most of the time in the range 1010 – 1030 kW with few periods in the range 980 – 1050 kW. It should be noted that most of the power supplies were not regulated, therefore the RF output power was sensitive to the variation of the main.

The screen grid rectifier with its crowbar was very sensitive to parasitic signals that can fire it without other reason.

Adding the 2nd and 3rd phases the duration of the tests was 1061 hours. The DIACRODE tube was operating at full power for 1047 hours and was stopped 18 times for fault reasons for a total shutdown period of 14 hours (availability of 98.7 %).

Most of the faults were due to:

- i. screen grid (10 of them)
- ii. other equipment of the test facility (8 of them).

Therefore about 95 % of these faults were not due to the tube. After each trip-off the tube could be restarted immediately without any difficulty and does not show any sign of degradation. None of these faults seems to have caused an internal damage to the tube.

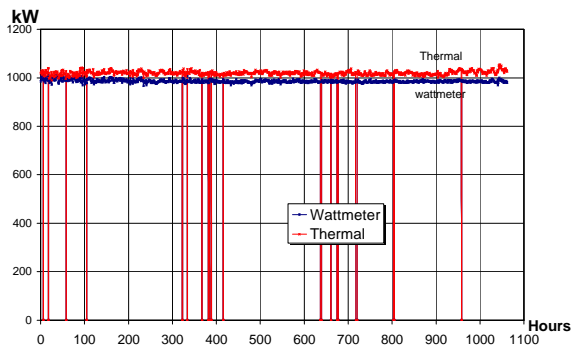


Figure 12: RF output power DIACRODE S/N 00102

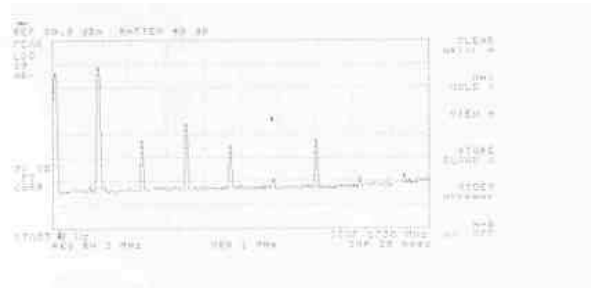


Figure 13: Output Spectrum on a calibrated probe

### 3.4 Conclusion

The conditions selected to make this test were the best ones. The cathode being cycled at each restarting. The tube was cycled in RF and temperature with short periods (65 hours) and long periods (220 hours).

The DIACRODE has shown its capability to run at 200 MHz at an output power over 1000 W with an operating point remarkably stable. This long test of 1047 hours demonstrated the great improvement brought by the new design of a power gridded tube and the feasibility of a RF tube in relevant IFMIF conditions (175-200 MHz 1MW cw).

In conclusion the tests foreseen in the contract were successful and the DIACRODE tube has shown the capability to operate at IFMIF relevant conditions (200 MHz – 1 MW CW) with a remarkably stable operating point.

The final report was submitted by Thales on 22 July 2002, well in advance compared to the contract completion date (31 October 2002).

The IFMIF accelerator does have at least one tube manufacturer.

Thales had and may again easily provide a budgetary evaluation for the IFMFI program.

### 3.5 References

EFDA Executive summary, Study contract FU 05 CT 2001 – 00135, (EFDA/00-926)

THALES Electron device, IFMIF tests final report, RP 511.02.049 ChR/pv, July 15, 2002

## 4 AC33A, AC38 -EU-CEA-Saclay: End to End beam dynamics

### 4.1 Brief task description

The IFMIF project (International Fusion Materials Irradiation Facility) requests two linacs designed to accelerate 125 mA CW deuteron beams up to 40 MeV. After extraction and transport, the deuteron beams with strong internal space charge forces have to be bunched, accelerated and transported to targets for the production of high neutrons flux. This task presents the reference design linac for this project. It is a combination of RFQ and DTL structure. Beams dynamics end-to-end calculations with errors studies and cavities design are detailed.

### 4.2 Contributors

Name	Party	Institute	E-mail address
R. Ferdinand	EU-FRANCE	CEA-Saclay	<a href="mailto:rferdinand@cea.fr">rferdinand@cea.fr</a>
R. Duperrier	EU-FRANCE	CEA-Saclay	<a href="mailto:rduperrier@cea.fr">rduperrier@cea.fr</a>
D. Uriot	EU-FRANCE	CEA-Saclay	<a href="mailto:duriot@cea.fr">duriot@cea.fr</a>

### 4.3 Introduction

IFMIF requires generation, by a linear accelerator, of 250 mA continuous current of deuterons at a nominal energy of 40 MeV, with provision for operation at 30 MeV and 35 MeV [1]. The basic approach is to provide two linacs modules, each delivering 125 mA to a common target. This approach has availability and operational flexibility advantages.

Very low beam loss along the linac is required in order that maintenance can be performed without remote manipulators. This study presents the reference design for the RFQ and DTL parts. Beams dynamics with and without errors are detailed. This work is done for the fusion community and supported by the EFDA contract 2000/10 .

### 4.4 RFQ design

The IFMIF 175 MHz RFQ is a four vanes structure. This ensures minimum power consumption compared to coaxial RFQs and a better control of the cavity deformations in CW mode. The cavity, designed with BELENOS [2], has a total length equal to 12.482 m and is segmented in three parts. This segmentation ensures an efficient longitudinal damping of the field errors [3]. It induces two resonant coupling gaps. The first gap is located at 4.161 m and the second one at 8.321 m. From mechanical considerations, in particular size of the welding furnaces, each segment is cut in four pieces of 1.04 m. Figure 14 and Figure 15 show 3D views of segmented RFQs [4,5]. The different parameters are summarized in table 1. It can be noticed that the final synchronous phase is  $-40^\circ$ . One may think that this value is too high and penalizes the accelerating efficiency of the structure, but this choice induces appreciable margins for the longitudinal acceptance. This point is important for such level of current. The high voltage (130 kV to 100 kV) compensates this high synchronous phase and allows a strong focusing.

Parameters	Values	Parameters	Values
Length	12.482 m	Synchronous phase	$-90^\circ \rightarrow -40^\circ$
Frequency	175 MHz	Peak field	1.8 Kp
Voltage	130 $\rightarrow$ 101.2 kV	Copper power	683.9 kW
Mean aperture ( $R_0$ )	6.41 $\rightarrow$ 5.16 mm	Beam power	613.1 kW
Modulation (m)	1. $\rightarrow$ 1.6	Total power	1297 kW

Table 1 : Main IFMIF RFQ parameters.

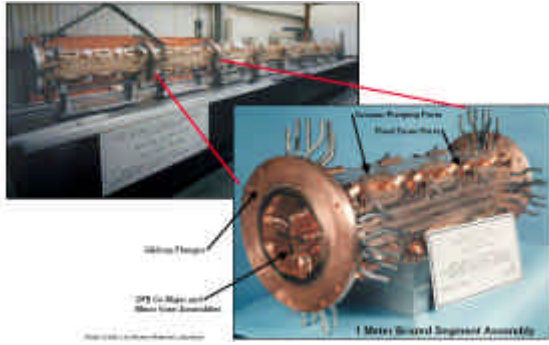


Figure 14 : Pictures of the LEDA RFQ

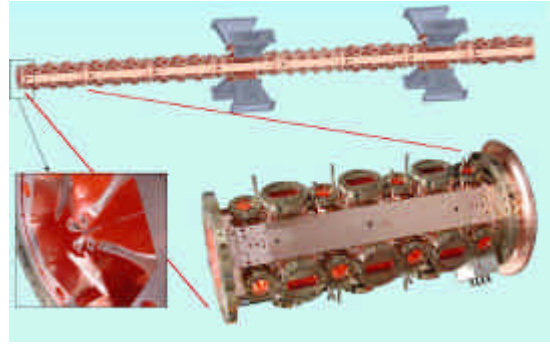


Figure 15 : Pictures and drawing of the IPHI RFQ

#### 4.4.1 RFQ Beam dynamics

In order to ensure the required 125 mA, a current of 130 mA is simulated in the RFQ. The input normalised rms emittance is  $0.25 \pi \cdot \text{mm} \cdot \text{mrad}$  at 95 keV. These values are in agreement with the present performance of SILHI [4], the French ECR source and the LEDA ECR source [5]. Table 2 shows the main results of simulation performed with the code TOUTATIS [6]. The output phase space distribution is plot in Figure 16.

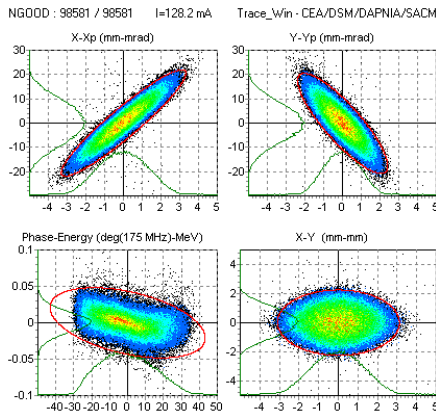


Figure 16 : IFMIF RFQ output phase space

Parameter	Value
Transmission	98.5%
Output X transverse emittance	$0.249 \pi \cdot \text{mm} \cdot \text{mrad}$
Output Y transverse emittance	$0.251 \pi \cdot \text{mm} \cdot \text{mrad}$
Output longitudinal emittance	$0.195 \text{ deg} \cdot \text{MeV}$

Table 2 : Results of the IFMIF RFQ simulation

#### 4.5 DTL design

The 175MHz DTL cavities have been designed with the GENDTL code [7]. The DTL part is comprised of 10 tanks. Each cell has been computed with SUPERFISH [8]. Main parameters (phase, field law) are computed by a step-by-step transport of a reference particle. Table 3 summarized the main parameters.

Table 3: Main parameters of IFMIF DTLs

Parameters	Values	Parameters	Values
Length (10 tanks)	31.8 m	Peak field	1.3 Kp
Max. $Z_s T^2$	$39.53 \text{ M}\Omega/\text{m}$	Copper power (+20%)	1907.1 kW
Maximum quad. gradient	74 T/m	Beam power	4550 kW
Synchronous phase ( $\Phi_s$ )	$-45^\circ; -35^\circ$	Total power	6.46 MW

##### 4.5.1 Beam dynamics

Figure 17 shows the behavior of x and phase beam distribution along the DTL tanks. No emittance growth and no loss are observed. The output current of 127 mA fills the IFMIF requirements with a small margin.

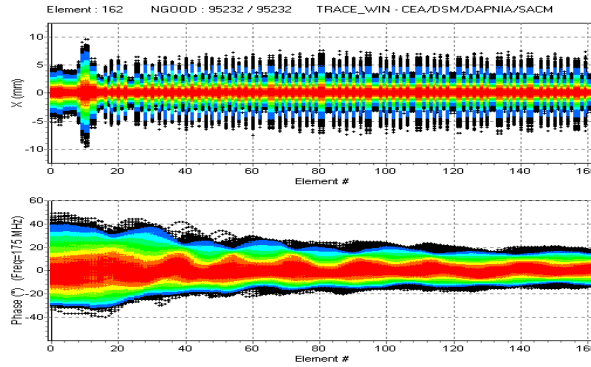


Figure 17 : X and phase beam distribution along DTL.

## 4.6 Errors Studies

### 4.6.1 Strategy

The study is decoupled, each defect being first studied separately. For example, the sensitivity on modulation error until a value of M was tested, the range [0→M] being cut in 10 steps: ten per cent of M, twenty per cent of M, ...For each step, 100 linacs are generated with a randomly distributed error. The longitudinal step on error is based on the machining step (IPHI RFQ) for each drawing. Once this first study is performed, it is then possible to extract from the simulation the maximum error amplitude for each defect.

Finally, all errors are combined with a maximum excursion, which has been determined in the first study. The combination is also cut in ten stages of 100 linacs. At the end, it is easy to determine the required threshold for each defect.

The GUI for errors studies is TraceWin [9]. User can easily choose errors types: phase, voltage, field, segment or tank tilt and misalignment...Calculations are distributed on several computers via a client/server architecture (multiparameters scheme) [10]. Ten PCs have been used for the IFMIF linac study during two weeks.

### 4.6.2 Results

For the RFQ cavity, the machining defect and misalignment have been studied separately. The machining defect is simulated with a wrong transverse and longitudinal curvature. Misalignments are segments tilts, rotations, and shifts. Figure 18 shows emittance and losses growth with respect to a fraction of the maximum machining defect (100  $\mu\text{m}$ ). It can be noticed that below 60  $\mu\text{m}$ , the performances are stable. The study for segment misalignments shows that a 120  $\mu\text{m}$  error is acceptable. The combined study decreases the tolerances to 50  $\mu\text{m}$  for machining and 100  $\mu\text{m}$  for misalignment.

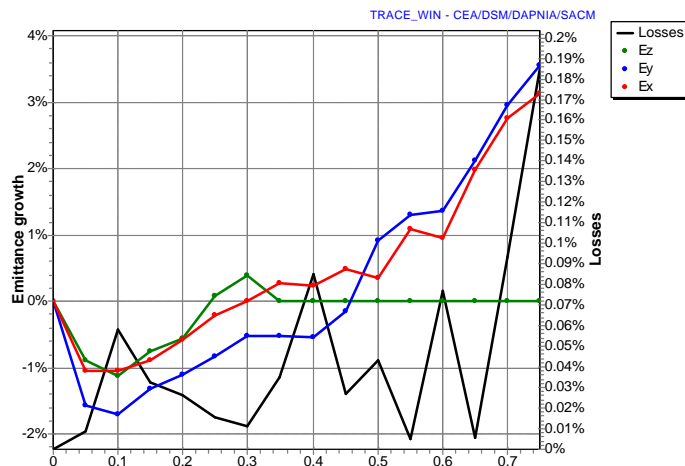


Figure 18 : Emittances and losses growth in respect to machining defect (fraction of 100  $\mu\text{m}$ ).

The DTL and matching line defects are quadrupoles errors (displacement and rotation in three directions, gradient). To correct beam misalignments, a couple of steerers are placed into the last tubes of each tank and a couple of Beam Position Monitor (BPM) are placed between tanks. A first errors study gives tolerances of 100  $\mu\text{m}$  for displacement, 0.25° for rotation and 1 % for the gradient.

Once each part has been studied, the whole linac is simulated. Figure 19 and Figure 20 show the beam size for 100 runs of 10 000 macro particles without and with combined errors and correctors. The red line corresponds to 90% of the beam; the blue to 99%, ... The black line includes all the beam. Figure 21 shows the output beam distribution in phase space for the two cases.

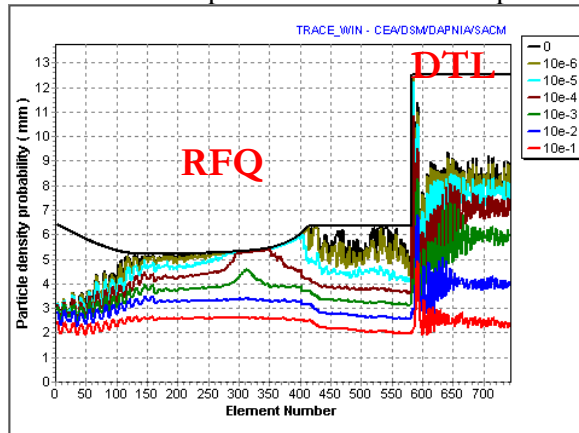


Figure 19 : Beam size along the accelerator without errors

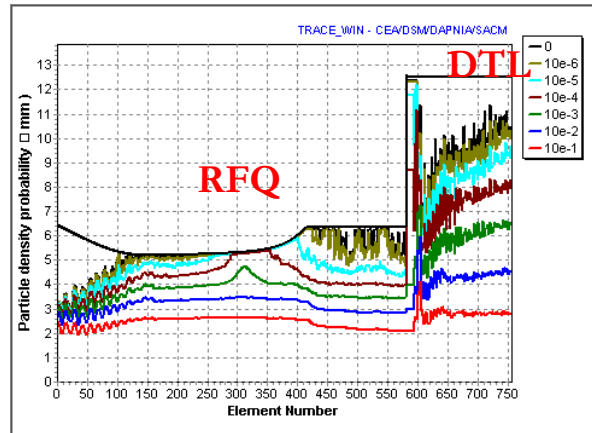


Figure 20 : Beam size along the accelerator with errors

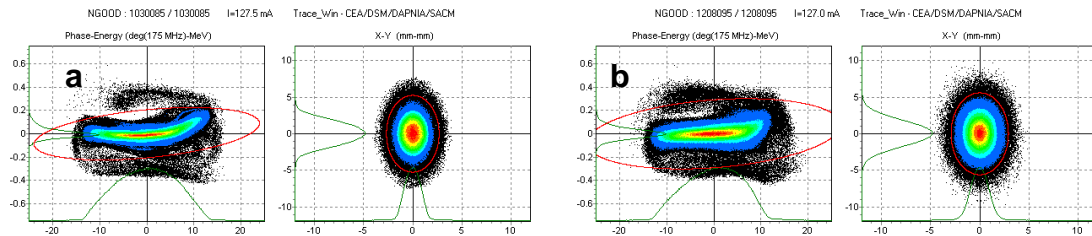


Figure 21 : Beam distribution in phase space at linac exit a) without errors b) with errors.

The rms emittance growths are 50% in the transverse planes and 14% in the longitudinal one. No extra loss is observed because of the errors due the efficiency of the correction scheme.

#### 4.7 Conclusion and perspective

The beam dynamics study showed no special concern. This reference design fulfils the IFMIF requirements. With errors and corrections, the transmission is expected to reach 98%. No loss occurs in the DTL part. This error study does not include input beam errors (beam mismatch, etc...), RFQ field errors, phase errors in the DTL and BPM readout errors.

A new design is under study, using 2 diacodes in the last 4 DTL tanks. One RF systems per linac is then saved. The overall efficiency is better and the errors studies are under investigations (there are less BPM and steerers). The results will be available before the end of 2002 and will also include all the above-mentioned errors (RFQ field, phase, BPM errors).

#### 4.8 References

- [1] IFMIF international team, "IFMIF key element technology phase, interim report", JAERI-Tech 2002-22.
- [2] R. Duperrier, "High intensity beams dynamics in RFQs", Ph. D. thesis n°6194, Orsay, July 2000.
- [3] L. Young, "Segmented Resonant Coupled RFQ", proceeding PAC 1993, Washington, D.C..
- [4] P.-Y. Beauvais & al., "Status Report on the Saclay High Intensity Proton Injector Project (IPHI), EPAC 2000 Proceedings.
- [5] H. Vernon Smith, Jr., J. D. Schneider, and R. Sheffield, "Low-energy demonstration accelerator (LEDA) test results and plans", PAC01, Chicago, pp 3296-3298.
- [6] R. Duperrier, "TOUTATIS, a radio frequency quadrupole code", Phys. Rev. Special Topics Acc. & Beams, december 2000.
- [7] D. Uriot, N. Pichoff, "GENDTL", internal report CEA/DSM/DAPNIA/SEA/2000/46.
- [8] J. Billen, L. Young, "Poisson Superfish", Los Alamos internal report LA-UR-96-1834 (1996).
- [9] D. Uriot, N. Pichoff, "TraceWin, Documentation", internal report CEA/DSM/DAPNIA/SEA/2000/45.

- [10] R. Duperrier, D. Uriot, N. Pichoff, “Cluster pour études d’erreurs de dynamique faisceau”, internal report CEA/DSM/DAPNIA/SACM/2002/21

## 5 AC34-EU-CEA-Saclay : RFQ Tuning method, Electric field optimisation on cold model

### 5.1 Brief task description

RFQs are powerful accelerators to both accelerate and bunch beams. Nevertheless, the IFMIF beam power and IFMIF RFQ design complicates the RF tuning of this part of the accelerator. The task will consist in using the IPHI RFQ cold model to develop the tuning method and the tools for the IFMIF RFQ RF tuning.

### 5.2 Contributors

Name	Party	Institute	E-mail address
R. Ferdinand	EU-FRANCE	CEA-Saclay	<a href="mailto:rferdinand@cea.fr">rferdinand@cea.fr</a>
A. France	EU-FRANCE	CEA-Saclay	<a href="mailto:afrance@cea.fr">afrance@cea.fr</a>
F. Simoens	EU-FRANCE	CEA-Saclay	<a href="mailto:fsimoens@cea.fr">fsimoens@cea.fr</a>

### 5.3 Studies

The building and the development of a complete RFQ tuning method [1] has implied 3 main parts:

#### 5.3.1 Test bench

An experimental test bench [2] has been designed and developed in order to measure the electromagnetic parameters to be tuned.

##### *Test bench principles*

The bench that measures the field distribution in the cavity is based on the perturbation method. The acquisition of the s21 transmission coefficient phase shift is synchronized with the displacement of a bead through the 4 quadrants of the RFQ. The measured raw data are then converted to a quantity proportional to the electromagnetic field magnitude. The overall set-up is fully computer controlled and easily transportable.

##### *Special topics*

The important efforts that have been devoted to the optimization of the signal to noise ratio have led to very sensitive and repetitive measurements; these characteristics are essential for an accurate RFQ tuning.

The technological choices of the experimental set-up are such that it can be directly applied to RFQ's having geometries or working resonance frequencies different from that of IPHI RFQ.

#### 5.3.2 Mathematical model

A comprehensive mathematical model [3] has been developed.

##### *RFQ model principles*

The RFQ is viewed as a Transverse Electric wave-guide at cut-off. The central region delimited by electrode tips is modeled by a coupled, inhomogeneous (i.e. the geometry and the cut-off frequency of the transverse section varies longitudinally) 4-wire line system. The shunt admittances are derived by stating a purely transverse propagation in the wave-guide, and series self- and mutual- inductances by stating a phase velocity equal to light velocity at infinite frequency. The voltages between electrodes are solution of a vector differential equation, which is recast into an eigen-value problem, leading to a bi-orthonormal basis and its associated inner product. The real RFQ is then viewed as a perturbation of a perfectly symmetrical RFQ, and the measured fields are expanded on the eigen-basis. Ends boundary conditions are of the von Neumann type, and are directly extracted from measured fields before expansion. The field perturbations are then transformed into line perturbations, such capacitance perturbations (continuous functions of abscissa) or tuners perturbations (discrete functions), for which eigen-bases are built, following the Riesz theorem

### *Different interpretations of the measured fields derived from the mathematical model*

The model is able to interpret the fields measured in a real-life RFQ in terms of :

- *Mechanical errors.* This theoretical approach leads to the estimation of the distribution of the transverse disequilibria between the 4 quadrants [4]. This diagnosis is able to check whether the mechanical structure of the RFQ sections has been modified by the brazing operation.
- *Slug tuners commands.* The mathematical model that has been developed for the IPHI project is continuous by nature, i.e. measured voltages are expanded on a set of continuous 'voltage basis functions', perturbed line inductances are expanded on a set of continuous 'inductance basis functions', with a one-to-one correspondence between the two sets, and a convergence theorem associated to these expansions. The tuning system of the RFQ (slug tuners) is on the contrary discontinuous by nature. Unfortunately, the sampling theorem that can be naturally derived from the reproducing kernel of the functional space is not directly applicable to an arbitrary, highly irregular distribution of tuners. An original anti-aliasing filter [5] is shown to yield a stable sampling of inductance functions belonging to a particular, but useful, sub-space. **The tuning of any segmented vane RFQ with the use of slug tuners is now theoretically modeled and computed.**
- *Ends detuning corrections by plate thickness and dipole rods lengths adjustments.* The two ends of the RFQ and the coupling cells (connecting each segment to the next one) are viewed as unknown circuits inserted in the 4-wire line model. The full set of electrical parameters of anyone circuit may be estimated from a set of measurements with various excitations of that particular circuit (excitation is varied by moving plungers some distance apart). End plate and coupling plate thickness are directly related to a few of these electrical parameters, quite suited for easy tuning. For dipole rods adjustment, a practical criterion derived from the theory has been introduced. This criterion ensures the convergence of tuning by preventing a too big discrepancy between the model and the real cavity [6].

### **5.3.3 Cold model testing**

The tuning formalism has been successfully tested on a RFQ prototype.

#### *RFQ cold-model*

A 6-m long aluminum RFQ cold model has been designed and built. In addition to being a very efficient and essential bench to validate the tuning formalism, this prototype has given the opportunity to test the validity of 3d electromagnetic codes simulations [7]. We remind that the design of the real RFQ is based on such simulations. In particular the vane-end matching is pretty well predicted: accurate field measurements on a 1-m long configuration showed excellent agreement vs. simulation with or without dipolar stabilizer rods.

A specific study has consisted in comparing measurements of segmented modes on the RFQ cold-model, with our mathematical model and 3d simulations results [8]. The good agreement that we have found validates our cut-off wave-guide equivalence approach.

Specifically for the RFQ tuning study, different transverse section positions where to guide the perturbing object have been tested on our RFQ cold-model [9]. This study has led to the choice of field measurement on the bisector of each quadrant.

#### *Different tuning procedures*

##### *1-Mechanical errors diagnosis.*

Tests of cold-model vane mechanical translations have demonstrated the ability to **detect displacements as small as 20 micrometers** [4]. Though being less precise than 3d mechanical measurement probes, this diagnosis of the mechanical defaults is very relevant since it can be applied inside the cavity even after its brazing. It has been decided to apply this test RF test on each single RFQ on the factory site before and after brazing.

During the year 2002, the first IPHI RFQ section defaults have been characterized on the factory site before and after brazing [9]. The measurement bench has been moved to the industrial site for the tests. These tests have shown that the brazing procedure had slightly modified one dipolar contribution while keeping its level very low.

##### *2- Slug tuners commands.*

The tuning slugs are highly irregularly spaced along the RFQ structure, between vacuum windows, RF wave-guide inputs and cooling ducts. The slug tuners commands [5] have been successfully tested for many configurations of the cold prototype, as a one-meter homogeneous line with eight tuners (per quadrant), a two-meter homogeneous line with eight tuners on the first meter and four tuners on the second meter, the same two-meter line, with a capacitive coupling cell at mid-position. This last case corresponds to the fact that the IPHI RFQ is segmented, i.e. the RFQ line is divided into four 2-meter long segments, with capacitive couplings in-between.

Modulated and non-constant  $r_0$  vanes have been installed in the body of the cold-model which simulates precisely the first 2-m long segment of the real IPHI RFQ. The voltage profile has been tuned with the IHI RFQ specifications (first 2 meters) using the algorithm and only slug tuners.

For all configurations, the tuning procedure requires only a small number of iterations, and convergence is demonstrated on every component of the functional bases. Constant and variable voltage profiles have been tuned in only 4 steps achieving a final relative voltage error better than 1% in every quadrant and at any longitudinal position.

3- *Dipole ends detuning corrections by rods lengths adjustments [6].* A ‘quadratic shift frequency’  $df(n)$  can be computed in all RFQs. By adjusting the rod length, the measured  $df(n)$  is made equal to the nominal value. When this criterion is satisfied, tuning tests of the RFQ cold-model using only the slug tuners have perfectly converged.

4- *Quadrupole ends detuning corrections by plate thickness adjustments [6].* The tuning of the ending regions with respect to the quadrupole mode is made by machining the thickness of the ending plates. The end region mismatch is characterized by a parameter  $W=LxDf$ , expressed in m.MHz, where  $L$  is the RFQ half-length and  $Df$  is the difference between mismatched and matched resonance frequencies. Our model can extract  $W$  from at least 3 measurements with different voltage excitations. These excitations are easily achieved by moving slug tuners at some distance of the end being tuned. The tests on the cold-model have shown very good agreement between the  $W$  sensitivity extracted from the measurements and the 3d simulations.



Figure 22: 6-m long IPHI cold model



Figure 23: Low level analyses before brazing.

## 5.4 Conclusion

The formalism that has been developed permits the computation of all quantities necessary to RFQ tuning procedures:

- plate thickness and dipole rods lengths adjustments (boundary regions),
- slug tuners commands.

It also generates a unique diagnosis of the mechanical defaults of each single RFQ section, available at factory site before and after brazing.

All these procedures have been validated on our cold model, with different configurations:

- with a constant or variable inter-electrode  $r_0$ ,
- in a homogeneous or inhomogeneous RFQ (i.e. with electrical parameters varying from one cell to the next),
- segmented or not,
- with a constant or variable accelerating voltage law,
- at different resonance frequencies of the accelerating mode,
- with different lengths.

The rigorous mathematical model makes possible a fast convergence and a high precision tuning level. **Its other important advantage is that it can be applied to all 4-vane RFQs, regardless of the resonance frequency, accelerating voltage profile and mechanical length.**

## 5.5 References

- [1] F. Simoens, 'Etude théorique et expérimentale du réglage électromagnétique d'une cavité radio-fréquence quadripolaire (RFQ) accélératrice d'un faisceau intense d'ions', Thesis of the 'Pierre et Marie Curie' University, September 2002
- [2] F. Simoens, F. Ballester, A. France, J. Gaiffier, A. Sinanna, "A Fully Automated Test Bench for the Measurement of the Field Distribution in RFQ and Other Resonant Cavity", EPAC2002 Conference (Paris), June 2002
- [3] A. France, F. Simoens, "Theoretical Analysis of a Real-life RFQ Using a 4-Wire Line Model and the Spectral Theory of Differential Operators.", EPAC2002 Conference (Paris), June 2002
- [4] F. Simoens, A. France, J. Gaiffier, "A New RFQ Model Applied to the Estimation of Mechanical Defaults Distribution", EPAC2002 Conference (Paris), June 2002
- [5] F. Simoens, A. France, J. Gaiffier, "A New RFQ Model applied to the Longitudinal Tuning of a Segmented, Inhomogeneous RFQ with Highly Irregularly Spaced Tuners", EPAC2002 Conference (Paris), June 2002
- [6] F. Simoens, A. France, "Tuning procedure of the 5 MeV IPHI RFQ", CEA-SACLAY, LINAC Conference (Gyungju, Korea), August 2002
- [7] P. Balleyguier, F. Simoens, "Simulations vs. Measurements on the IPHI RFQ Cold Model", EPAC2002 Conference (Paris), June 2002
- [8] F. Simoens, A. France, O. Delferrière, "An Equivalent 4-Wire Line Theoretical Model of Real RFQ based on the Spectral Differential Theory", CEA-SACLAY, LINAC Conference (Gyungju, Korea), August 2002
- [9] F. Simoens, A. France, J. Gaiffier, "Electromagnetic Characterization of the First IPHI RFQ Section", EPAC2002 Conference (Paris), June 2002

## 6 AC36-EU-CEA-Saclay : Drift Tube Linac R&D Studies

### 6.1 Brief task description

The task was completed in the framework of the CEA program on high-power particle accelerators supported by the IPHI demonstrator project. This project is dedicated to high power beam production. Drift tube and quadrupoles analyses include cavity calculations, power deposited, and extrapolation from IPHI DTL measurement on hot model (measured power deposition, cooling, manufacturing tolerances...).

### 6.2 Contributors

Name	Party	Institute	E-mail address
R. Ferdinand	EU-FRANCE	CEA-Saclay	<a href="mailto:rferdinand@cea.fr">rferdinand@cea.fr</a>
P-E. Bernaudin	EU-FRANCE	CEA-Saclay	<a href="mailto:pebernaudin@cea.fr">pebernaudin@cea.fr</a>

### 6.3 Introduction

A 4-cells short hot model of a 352 MHz drift tube linac has been built in CEA Saclay. The purpose of this model is to verify the feasibility of such a structure for cw operation with a high current beam inducing tight tolerances.

This short model includes one tank, three drift tubes of two different designs and two magnets of different types. Their designs have been described in [1] and are summarized below.

The main difference between the IPHI and IFMIF DTLs is the frequency. Generally speaking, the higher frequency of the IPHI DTL is more restrictive as the dimensions are smaller, especially for the first drift tubes and magnets for which the dimensions problems are more sensible. Therefore, results obtained for the IPHI DTL can be easily extrapolated for the IFMIF one, with even a safer margin. From a manufacturing point of view, dimensions are not different enough to lead to different problems and solutions. And more important, both machines share the more constraining aspect, which is the cw operation mode.

### 6.4 Magnets

The magnets (Figure 24) are made of two different materials, one in standard soft iron, and the other in cobalt-iron Permendur alloy. They are optimized so as to provide the strongest integrated transverse gradient with the smaller power dissipation, respecting a 0.5% homogeneity tolerance over the useful region (a circle of 6.5 mm radius). Their main characteristics are summarized in Table 3. The cooling scheme of both magnets is different. The Permendur electromagnet leads are standard hollow copper conductors, while the soft iron magnet's ones are not hollow, the cooling being external: the drift tube is flooded with water, which cools simultaneously the magnet leads and the drift tube walls. This scheme allows to enlarge slightly the magnet, and also to optimize the power dissipation (two layers of conductors against only one for the other magnet), leading to power dissipation 35% lower than for the more standard magnet. However, both magnets are strongly saturated.

	Permendur magnet	Soft iron magnet
Integrated gradient	4.70 T	4.70 T
Transverse gradient	83.79 T/m	75.89 T/m
Magnetic length	56.09 mm	61.94 mm
Total length	48 mm	56.16 mm
Pole length (beam axis)	36 mm	42 mm
External diameter	140 mm	157 mm
Aperture diameter	16 mm	16 mm
Amperes-turns	2 750	2 317
Turns per pole	5.5 in 1 layer	9 in 2 layers
Leads dimensions	5x5 mm	5.6x2 mm

Isolation	0.25 mm per face	0.07 mm per face
Intensity	500 A	258 A
Current density	27.88 A/mm <sup>2</sup>	23.04 A/mm <sup>2</sup>
Total resistance	6.1 mΩ	15.3 mΩ
Electric power	1 524 W	1 018 W
Nominal cooling flow	1.68 l/min	(External cooling)
Water heating	13°C	
Pressure drop	6.22 bars	

Table 3 - Quadrupole magnets data (as calculated)

The manufacturing process of these showed no major concern, except for the Permendur model. In this case, the yoke passage of the leads is very difficult considering the conductors dimension, the high degree of saturation (even in the yoke) and the small space available. This aspect led to drift tube welding problems, and it proved necessary to cut in the yoke at the prize of a performance decrease caused by the high saturation (3% on the transverse gradient, about 2.5% on the integrated gradient). Preliminary tests showed that the cooling was adequate, especially for the soft iron (flooded) model. On the other hand, some isolation defects between conductors and ground potential were detected in both models. The reasons of these defects are different for each magnet, but in each case causes are well established and solutions identified.

The magnets gradients have been measured<sup>1</sup>. The results for the soft iron magnets are as planned. In the Permendur magnet case, the modification performed on the yoke to ease the leads passage resulted in a 2.5% decrease of the integrated gradient at the nominal excitation.



Figure 24 - The magnets manufactured for the DTL short model. Left: Permendur magnet, right: soft iron magnet.



Figure 25 - Test piece of the transparent welding for the AES drift tube (interface between the three concentric stems and the drift tube two-parts body).

## 6.5 Drift tubes

Each magnet got a different drift tube design. The design intended for the Permendur magnet was performed by AES [2]. It is conventional, made of copper welded by the electron beam method. Coaxial stems guide the water in the drift tube where the cooling is located at the circumference only (two opposed azimuthal flows). This is the major weakness of this design, as the drift tube's other surfaces are cooled by conduction only, through the thin walls of the drift tube. Another problem is the complexity of the design, especially at the flow diverter level. This diverter is the piece which transforms the coaxial water circulation of the stems into the azimuthal circulation in the drift tube. A transparent welding is necessary to ensure watertightness at this level (Figure 25).

The other drift tube uses basically the same scheme (copper, coaxial stems, electron beam welding) but on a simpler scale. The whole drift tube being flooded, pieces and welding are less numerous. The complex diverter is not used. The stem is made of only two tubes, the magnet leads being cooled by the return flow. Advantages of this solution are numerous: mainly, cooling is better as almost every

<sup>1</sup> By Yorck HOLLER & al., DESY, Hamburg, Germany.

surface is directly in contact with the coolant, and the mechanical design is simpler, easier to manufacture, and therefore cheaper.

Several problems were raised during the manufacturing process. The first was the one related to the yoke passage of the Permendur magnet leads, as mentioned previously. This problem forbade the welding of the diverter on the body and forced us to modify the magnet's yoke to enlarge the leads passage at the magnet's magnetic performance expense.

Leaks appeared in both drift tube models (but more acutely in the non-flooded design) after the final machining. These leaks are related to an excessive thickness of the rough shape. An optimization of this thickness will allow to suppress this leakage problem.

## 6.6 Tank design

The high power density on the walls in such a cw machine makes the cooling a major concern, the ultimate purpose being to minimize and control both thermal stress and expansions. Another aspect is that the tolerances for the whole machine are very tight, because of the beam intensity and the focusing type (FODO). Therefore the tolerances are especially strong for the magnetic alignment of the quadrupoles (IPHI:  $\pm 51 \mu\text{m}$  misalignment, gradient  $\pm 0.5\%$ , IFMIF:  $\pm 100 \mu\text{m}$ , gradient  $\pm 1\%$ ). The design is further complicated by the very short space between successive drift tubes.

Despite theoretically not unsuitable, a full copper solution is extremely costly and should be used only when no other solution is available. The solution used for the hot model tank is a stainless steel thin (4-mm) envelope, which is copper-plated both inside and outside by an electrolytic process. The inner plating is obviously for electric conductivity purposes, whereas the thicker external plating is intended to enhance the thermal conductivity of the envelope. With a 1-mm thick external layer, the maximum temperature increase on the tank walls is divided by more than 4 (both plating being done almost simultaneously). Other technical solutions, like a thermally sprayed copper coating, have been studied.

The non-welded elements of the cavity (caps and girder, see below) are full OFHC copper parts.

The mechanical design of the cavity, and especially of the apertures (vacuum pumping slot, RF coupling, girder aperture) have been optimized to minimize thermal stress. Thermal displacement have been computed and will be measured during the test phase.

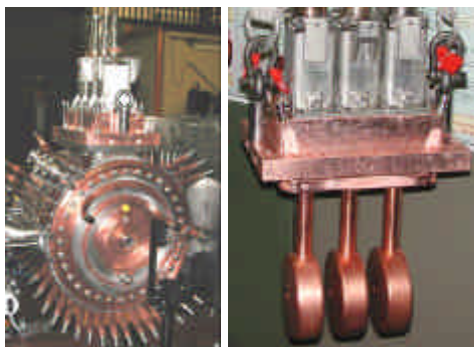


Figure 26 - Left: the hot model fully assembled. Right: girthing supporting the three drift tubes.

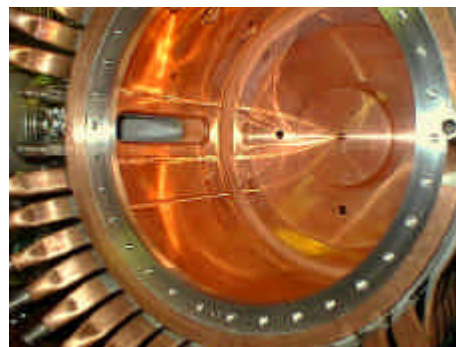


Figure 27 : interior view of the copper-plated stainless steel tank (the aperture is the pumping slot).

Great care has also been devoted to the optimization of the stem - tank connection, which proved to be a sensitive point in previous cw DTL projects (namely Chalk River and Los Alamos' FMIT). A flexible system based on a thin copper bellow allows mechanical adjustment of the drift tube position and orientation (except around the stem's axis) at any time. Mechanical tests have been performed on a bellow to ensure the vacuum tightness.

The tank design is both cheap and reliable, presenting no major difficulty. Copper plating has been made using the acid bath technique which, according to measurements performed, yields the lower outgasing rate and, according to bibliographical sources, the best RF electrical conductivity. The length of each tank section will therefore be limited by the plating bath dimensions, the biggest ones being GSI's with a depth capacity of up to three meters.

## 6.7 Hot model tests

Power tests have been limited by the inability of the CERN to provide the required power (40 kW cw). Up to now, only 8 kW cw have been available (but more than 50 kW peak power at low duty cycle). Further work is being performed on the power amplifier in order to solve this problem.

Within this power range, some results have nevertheless been obtained.

The Q factor of the cavity (21600) is 1/3 lower than the calculated *SUPERFISH* value. This result is worse than expected, but the relative effects of the cavity edges and of the various apertures (pumping, RF coupling, diagnostics) are very important. The strong influence of RF seals has been measured (the suppression of the girder RF seal alone leads to a 15% decrease of the Q factor.)

The low level rf tests allowed us to measure the on axis field and showed the benefits of the shift possibility of the drift tube positions.

Globally, no major heating has been discovered. All measured values are coherent with respect to the expected ones, at least at this level of rf power. Nevertheless, we were not able to measure any displacement, most probably because of this low level of power.

The electric field on the axis was measured under RF operation using a X-ray spectrometry measurement technique (the RF was pulsed in order to perform measurements up to 40 kW, peak power). The results of these measurements confirm that the Q factor is 1/3 lower than expected by *SUPERFISH*. The precision of the X measurements technique is estimated to be 3%.

RF conditioning was quite easy up to the reached powers (55 kW peak power, 8 kW mean power), with a good enough vacuum and very few observed multipactor level. The nominal vacuum seal configuration (*Helicoflex* seals) has not yet been tested.

## 6.8 Perspectives

Further tests will be carried on as soon as the RF amplifier will be ready. The cavity will be tested at nominal cw power from the thermal, mechanical and vacuum point of view.

Useful information has been gathered all along the manufacturing and test phases, that allows us to contemplate the construction of a cw DTL in a relatively close future. Different engineering designs for magnets and drift tubes have been put into operation, leading to several possible improvements.

One is also looking for solutions to relax the excessively strong tolerances imposed on the magnet alignment, mainly by increasing the beam aperture.

## 6.9 References

- [1] "CEA-DSM-DAPNIA-SEA contribution to the IFMIF KEP phase. Step report – June 2001". DSM/DAPNIA/SEA 01/41, 35 pages.
- [2] Advanced Energy Systems, Inc., "Conceptual design development of the 5 MeV drift tube for the IPHI drift tube linac - Phase I final report" (23/04/1999).
- [3] P.-E. Bernaudin & al., "Design of the IPHI DTL", Proceedings of the 2001 Particle Accelerators Conference.
- [4] P.-E. Bernaudin, O. Delferrière, M. Painchault, "Technical innovations for a high gradient quadrupole electromagnet intended for high power proton drift tube linacs", Proceedings of the 2001 Magnet Technology (MT-17) Conference.
- [5] M. Painchault, P.-E. Bernaudin, G. Congretel, "Thermo-mechanic of a DTL vessel for the IPHI project", Proceedings of the 2002 European Particle Accelerators Conference.
- [6] P.-E. Bernaudin, "Etude et optimisation d'un linac à tubes de glissement pour accélération de forts courants de protons en continu", PhD thesis of the Paris XI (Orsay) University, ref. 6975 (30/09/2002).
- [7] D. Uriot, N. Pichoff & P.-E. Bernaudin, "Design of a ramped-gradient drift-tube linac", CEA internal report ref. DSM/DAPNIA/SEA 2000/69 (12/12/2000).

## 7 AC41-EU-CEA-Saclay : Diagnostics for high power beam

### 7.1 Brief task description

The task was completed in the framework of the CEA program on high-power particle accelerators supported by the IPHI demonstrator project. This project is dedicated to high power beam production. IFMIF beam represents about 15 kW between the source and the RFQ, 625 kW before the DTL and 5 MW in the HEBT. The relatively low energy (40 MeV) means that this power is deposited in any interceptive diagnostics. New kind of diagnostics has to be developed, including intensified CCD analyses, spectroscopy analyses, pulsed wire scanner, laser analyses...

### 7.2 Contributors

Name	Party	Institute	E-mail address
R. Ferdinand	EU-FRANCE	CEA-Saclay	<a href="mailto:rferdinand@cea.fr">rferdinand@cea.fr</a>
P. Ausset	EU-FRANCE	CEA-Saclay	<a href="mailto:ausset@ipno.in2p3.fr">ausset@ipno.in2p3.fr</a>

### 7.3 Introduction

Among the parameters needed to be measured for beam control, monitoring and halo formation prevention, the transverse beam profiles are the most difficult to obtain. The large expected specific energy deposition in any interceptive monitor can lead to the destruction of the sensor and in addition to an appreciable amount of radiation production. Therefore traditional multi-wires chambers and wire scanners are not usable under too high duty factor pulsed-beam operation and obviously continuous beam operation.

A very attractive phenomenon is the production of visible light by the beam to background or additional gas interaction. Transverse beam profiles of the SILHI ECR source have been measured. However, several difficulties emerge to explain the difference shape between the transverse beam profiles deduced from the elementary observation of the emitted light by a CCD camera, a grid profiler (low duty cycle operation) and a residual gas profiler, respectively. More sophisticated measurements using the Doppler effect have been brought into operation to determine the energy and the spatial extension of the different components of the beam.

Wire scanners are also usable under low duty factor pulsed beam operation. Experiments have been conducted on tungsten, tantalum, titanium and carbon wires intercepting a 5 MeV proton beam delivered by the TANDEM accelerator of the Institut de Physique Nucléaire d'Orsay. Transverse beam profiles have been deduced from back-scattered protons, X and  $\gamma$  emission and electric current collected in the wires.

### 7.4 Optical measurement

In the LEBT the moderately relativistic protons interact strongly with the atoms of the residual gas which is mainly hydrogen (pressure  $2 \cdot 10^{-5}$  hPa). A blue light, visible by the human eye, is emitted by the de-excitation of these atoms. This light was first sensed with an intensified CCD camera working in the 200 nm-820nm range.

#### 7.4.1 Fluorescence Beam Profile Measurements (FBPM) Under CW and Pulsed Mode Operation

The experiments were carried under CW and pulsed mode operation in a diagnostics box, located after the two solenoids focusing the beam in the LEBT line. Other gases such as N, Ne, Ar, Kr, Xe, We were injected inside this box in addition to the residual gas. Two intensified 16-bit CCD cameras were installed perpendicularly to the axis of the beam, in order to measure vertical and horizontal beam profiles. Specific software performing the subtraction of the background signal (without beam) to improve the signal/noise ratio, the calculation of vertical and horizontal projection and peak fitting convolution were used. It has been found:

- The proton beam is, as expected, cylindrical along the LEBT
- The intensity of the emitted light depends on the nature of the gas and increases proportionally to the pressure of the gas.
- Profiles obtained by FBPM have the same geometrical shape for all gases at the same pressure (after normalisation with respect to the amplitudes of the profiles). The same result is obtained for a classical grid profiler working under pulsed mode operation.
- Under pulsed mode operation, the widths of the profiles measured by FBPM are larger than the ones measured by a grid profiler (Figure 28). The width and the difference decrease as the pressure increases.

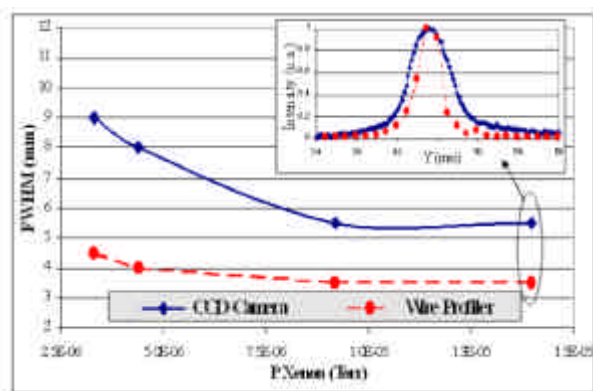


Figure 28: Evolution of the widths of the profiles measured by a grid profiler and by FWHM with the pressure of the gas (Xenon).

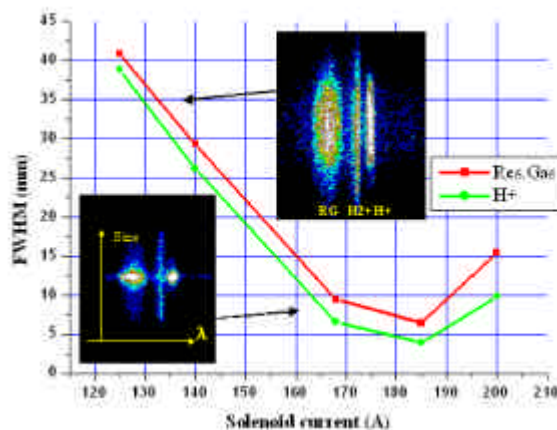


Figure 29: FWHM of the H $\alpha$  (residual gas) and its corresponding Doppler shifted line vs beam size (solenoid setting)

## 7.4.2 Spectroscopic Measurements

We replaced the horizontal CCD camera by a Photomultiplier coupled to a scanning monochromator in order to analyse the emitted light spectrum. As expected we found again the well-known lines of the Balmer series. Previously [3], precise measurements were made and showed that the amplitude of each line is proportional to the intensity of the proton beam. The light spectrum of the other gases (N, Ar, Kr, Xe, Ne) were also recorded. Experiments were carried out with a laser absorption on specific lines of Ar ( $\lambda = 811.5$  nm) and Kr (811.3 nm) with the aim of measuring the transverse profiles of the beam.[3,5]

## 7.5 Shifted doppler fluorescence beam profile measurements (SDFBPM)

The existence of a halo surrounding the core of the beam measured by FBPM suggests that the light produced by the excited atoms of the gas does not result only from the incoming protons, but also from second step processes involved in the production of this light.

Trying to explain the intensity and the spatial extension of the light produced in the vessel needs to consider several major physical processes which may contribute to the production of this light and to the broadening of the measured profiles:

- Possible delayed decay of excited atoms of specific gas present in the vacuum vessel (Nitrogen is well known for this phenomenon).
- Back scattered protons may also excite other atoms of the gas which lead to the production of light
- Inelastic collisions may produce electrons able to excite in their turn atoms of gas.
- Dissociation of molecules of H $_2^+$  and H $_3^+$  unfortunately produced by the source SILHI in addition to the protons may occur and create excited atoms which become source of light.

As we want to discriminate only the light produced by the incoming protons delivered by the source at 95 keV, and accelerated back-stream by the RFQ, we turn around to their high electronic capture cross section: A part of these protons captures in flight an electron and may give birth to excited hydrogen atoms. The typical Doppler shift effect of these very specific atoms in the frequency (or wavelength) domain will allow us to select their light produced by de-excitation among the overall light in the vessel.

### 7.5.1 Experimental Set Up

The CCD Camera was installed in the focal plane of an imaging spectrograph equipped with a 900 gr/nm grating. The resolution was better than 0.1 nm at 500 nm. The experimental configuration was chosen to shift sufficiently (8 nm) the  $H_{\alpha}$  line of the Balmer series of hydrogen.

The vertical beam profiles, according to the vertical slit orientation at the entrance of the monochromator, are deduced from the image transported on the CCD matrix of the camera.

In addition, due to the possible discrimination of the different components of the beam  $H^+$ ,  $H_2^+$  and  $H_3^+$  because of their different Doppler shift wavelengths, this method potentially allows:

- The relative intensity measurement of the different species present in the beam.
- The measurements of the transverse profiles of the species, which contribute to the entire profile of the beam.
- The energy measurements of the different species and in particular their energy spread which is proportional to the width of the corresponding spectrum line.

### 7.5.2 Experimental results

Identification of the different lines of the Balmer series of hydrogen were first recorded. Their corresponding Doppler shifts were checked. Secondly, the current in the solenoids were changed in a large range to vary the size of the beam. The full width half maximum (FWHM) of the ( $H_a$ ) and its corresponding Doppler shift line  $H_+$  component profiles were measured. A remarkable result is that the size of the halo surrounding the beam remains constant whatever the focusing conditions (Figure 29).

The evolution of the profiles was also studied varying the nature and the pressure of the gases introduced in the vessel: N, Ar, Kr, Xe, Ne and H. Adding gas into the vessel increases the produced light: for each component  $H_a$ ,  $H^+$ ,  $H_2^+$ ,  $H_3^+$  the fluorescence yield increases linearly with the pressure (up to  $10^{-4}$  hPa), except for hydrogen. The curve shows a saturation which may be attributed in a first time to an auto absorption process but this needs to be confirmed.

### 7.5.3 Absorption techniques

Absorption techniques were tested using laser light. Different injected gas (krypton, Argon with  $\lambda=811.5\text{nm}$ ) allow to observe a linear absorption with beam current and pressure. Nevertheless this technique did not give satisfactory results. As absorption was observed out of the beam, no direct profile was possible. Structures inside the measurement were observed and were not clearly understood. Metastable out of the beam due to excitation by fast electrons (...50eV) and diffusion are probably the reason of the difficulties.

## 7.6 Interceptive profile measurement methods

The machines are usually able to work under pulsed mode operation for machine commissioning and experimental operation. The beam average power reaches 15 kW at the entrance of the RFQ (95 keV) and 625 kW at the exit. Wire scanners are also usable under low duty factor pulsed beam operation.

### 7.6.1 Slow Wire Scanner (SWS)

In this method, a wire is stepped in small increments through the beam. The profiles are obtained over many pulses by measuring the current flowing in the wire resulting from the secondary electrons emitted from this wire, subtracted from the protons collected by this wire. The heating of the wire is the major problem because of the large energy deposited by the beam in any intrusive sensor. A crude estimation of the attained temperature is given by the resolution of the heat equation: The pulse

duration must remain below 300  $\mu\text{s}$  and the repetition rate above 1 s in order to maintain the peak temperature of a carbon fiber (30  $\mu\text{m}$  diameter) below 1200°K in a 5 MeV, 100 mA, 320 mA/cm<sup>2</sup> proton beam. SWS are only usable under low duty factor operation.

In the case of slightly higher beam average powers, the amplitudes of the mechanical deformations increase and thermo-ionic emission of electrons occurs which distorts the measurements of the true profiles. At higher beam average power and under CW mode operation any kind of fiber is destroyed.

### 7.6.2 Fast Wire Scanner (FWS)

At high average power pulsed beam and under CW operation, the wire must go very quickly through the beam. It was found that the speed of the wire must then exceed 60 m/s to withstand the power of a CW, 5 MeV, 100mA; 320 mA/cm<sup>2</sup> proton beam. Because of this high speed, a FWS is very difficult to design.

## 7.7 Experiments with wire scanner.

Even under low duty-factor pulsed-beam, the heating of the wire of SWS may bring out errors in the profile measurements in particular because of the thermo-ionic emission of electrons. In order to design a SWS, and to crosscheck the measurements of the current traditionally used in SWS, we looked for physical processes, the characteristics of which does not depend on the temperature.

Valid candidates are:

- The production of back scattered protons due to elastic collisions between the protons of the beam and the atoms of the wire.
- The production of  $\gamma$  (and X) ray due to the excitation or nuclear reaction of the nucleus caused by inelastic collisions between the accelerated protons with the atoms of the wire.

### 7.7.1 Experimental Setup

The tests were carried out on the TANDEM accelerator of the “Institut de Physique Nucleaire d’Orsay” in a 5 MeV and 1  $\mu\text{A}$  proton beam. A frame on which different samples of wire were fixed can be translated through the vacuum vessel. The current flowing in the wire was measured by a current to voltage converter, the current of the beam with a Faraday cup.

The amplitude of the pulse delivered by the charge amplifier associated with the Si junction is proportional to the energy deposited by the back-scattered protons. The transverse beam profiles are deduced by integrating the whole spectrum for each position of the wire. The same is done for the detection of the  $\gamma$  ray after detection with a NaI scintillator associated with a photo-multiplier. At last specific software was used to fit the measured profiles.

### 7.7.2 Experimental Results

Wires of different nature and diameters were tested: W ( $\phi= 100\mu\text{m}$  and  $500\mu\text{m}$ ), Ta ( $\phi= 100\mu\text{m}$ ), Ti ( $\phi= 125\mu\text{m}$ ,  $500\mu\text{m}$ ), C ( $\phi= 1\text{mm}$ ) and Ti wires. ( $\phi= 125\mu\text{m}$ ,  $500\mu\text{m}$ ).

- It was first checked that the profiles measured with the different wires were similar and did not depend on the diameter of the wire.
- For example, the profiles deduced from the backscattered protons, the  $\gamma$  ray production and the current measured with the Ti wire are very similar.

The first experiments show a very good agreement in the profiles measured with the different wires independently of the physical processes involved in the measurements. The total error in the measurement of the width is in the order of 250 $\mu\text{m}$ .

The obtained profiles are resulting of 5MeV particles, allowing the decorrelation of accelerated particles from background-ionised particles or non-accelerated particles coming through the RFQ. Halo measurement of real beam should be made possible with this technique (providing sufficient sensibility).

## 7.8 Conclusion

We developed specific tools for the measurement of the transverse profiles of high power proton beam.

- Under low duty factor pulsed beam operation traditional wire scanner work.
- Measurements of back scattered protons or  $\gamma$  ray production are powerful tools to cross check the measurement of the current in the wire in the temperature range of the wire below thermionic emission. Measurements by means of a wire scanner may be also cross checked with Doppler fluorescence beam profile measurements.

Because of their non destructive nature with respect to the beam, optical methods are very attractive for high power beam monitoring. We investigated and brought into operation some specific optical diagnostics on the high intensity source SILHI.

- Direct fluorescence beam profile measurements under high average power beam pulsed mode and CW operation are valid for centroid beam position measurement. In addition the qualitative estimate of the beam transverse profiles is possible.
- Fluorescence measurements on the Doppler shifted lines of the hydrogen Balmer series are very promising to determine the energy of the different components of the beam ( $H^+$ ,  $H_2^+$  and  $H_3^+$ ). In addition, the energy spread of the beam is potentially measurable. Beam profiles measurements are underway.

## 7.9 References

- [1] "CEA-DSM-DAPNIA-SEA contribution to the IFMIF KEP phase. Step report – June 2001". DSM/DAPNIA/SEA 01/41, 35 pages.
- [2] "CEA-DSM-DAPNIA-SEA contribution to the IFMIF KEP phase. Step report – June to December 2001". DSM/DAPNIA/SEA 02/09, 25 pages.
- [3] B. Pottin and al, "Optical beam profiler for high current beams" EPAC 2000, Vienne, June 2000
- [4] D.Gardès and al, "Optical beam-profile monitoring developed for high intensity proton beam" presented at 14<sup>th</sup> International Symposium on Heavy Ion Inertial fusion, Moscow, May 2000. To be published in Laser and Particle Beam.
- [5] B. Pottin, "Etude d'un Profileur Optique de Faisceaux Intense de Protons par Absorption Laser", These Université Paris XI, 18 Octobre 2001.
- [6] P. Ausset, S. Bousson, D. Gardes, A.C. Mueller, B. Pottin, R. Gobin, G. Belyaev, I. Roudskoy, "Transverse Beam Profile Measurements for High Power Proton Beams", EPAC 2002, La villette PARIS 2002, page 245
- [7] P. Ausset, S. Bousson, D. Gardès, A.C. Mueller, B. Pottin, R. Gobin, G. Belyaev, I. Roudskoy, "Optical Transverse Beam Profile Measurements for High Power Proton Beams", EPAC 2002, La villette PARIS 2002, page 1840
- [8] P. Ausset and al, "Beam diagnostics for high intensity accelerators", Workshop on utilisation and reliability of high power proton accelerators, Aix en provence, France 22-24 November 1999. (N.E.A.)